STUDY OF HEAT TRANSFER ENHANCEMENT OF DRAG REDUCING SURFACTANT SOLUTIONS THROUGH THE USE OF STATIC MIXERS

A THESIS

Presented in Partial Fulfillment of the Requirements for

Graduating with Distinction from the Honors Program in

Chemical Engineering from The Ohio State University

By

James Courtney Knight

*****

The Ohio State University

2009

Honors Examination Committee:

Dr. Jacques L. Zakin

Dr. James F. Rathman

THE OHIO STATE UNIVERSITY

College of Engineering
Engineering Honors Committee
Graduation With Distinction
Record of Oral Defense

This is to certify that James Knight has undergone the required examination* for Graduation With Distinction and that the quality of both the written and oral work is such that he/she should be graduated With Distinction in Chemical Engineering.
(Degree Program Name)

Sincerely,
Faculty Examiners

(signed) _____

(signed) _____

May 11, 2009
Date

* The final honors examination may include a written component but must include a one-hour oral examination before **two** members of the faculty with graduate advising status, one of whom is the thesis advisor. Both must sign the report form above. The signed report form is due to the college (Dave Donley) by the **end of the 7th week** of the quarter of graduation.

* The final thesis must be filed electronically with the Knowledge Bank by the end of the eighth week of the quarter of graduation.

Acknowledgements

I would like to thank my research advisor, Dr. Jacques Zakin for his patience and guidance with me on this research project. There was slow progress in the beginning with experimental setup and calibration, but he was very flexible about this. I would also like to thank Haifeng Shi as he helped me out the most with this project. He brought me up to speed on the experimental setup, the experimental procedure, and how to handle the data. He was also incredibly helpful by running some of the lengthy tests when I had class and other commitments that kept me from finishing them. Yi Wang also helped out by running a few experiments and providing an extra set of hands. I would also like to thank Wu Ge for his work on the project as well. He was a graduate student under Dr. Zakin, and he was responsible for much of the work required to get the experimental setup working. Dr. Richard Christensen also was kind enough to stop by and give us advice on how to improve our experimental setup through further calibration. I would also like to thank Leigh Evrard for fixing the many technical problems we had with the experimental setup. This included installing new parts, troubleshooting setbacks, and improving the data acquisition system. Finally, I would like to thank Dr. Rathman for agreeing to be part of my Honors Examination Committee despite his busy schedule.

Introduction

Drag reduction is the phenomenon in which adding a small amount of a chemical additive to a flowing fluid reduces the friction factor of the turbulent flow. This translates to an increase in flow rate at a constant pressure drop or a decreased pressure drop at a constant flow rate. Drag reducing agents can lead to reduced pumping energy requirements, fewer pumps required, or smaller pumps, all of which translate into reduced operating and/or capital costs.

The two most commonly used classes of drag reducing agents are high polymers and surfactants. High polymers permanently degrade under high shear stress, whereas surfactants are able to repair themselves through self-assembly after experiencing a period of high shear stress. Because of this ability, surfactants are the drag reducing agents of choice in systems that require recirculation.

Because drag reduction is a reduction in momentum transfer, a corresponding reduction in heat transfer is also experienced by the system. Depending on the application of the drag reduced system, this can be a beneficial or detrimental side effect. An oil pipeline that is heated to improve fluid flow is an example where this behavior is beneficial. A district heating and cooling system, where water is heated or cooled at a central location and then piped to nearby buildings for temperature regulation is an example where reduced heat transfer is harmful to system performance.

Several different methods have been proposed and investigated for improving the heat transfer properties of drag reducing solutions. All of these methods alter the chemical structure of the drag reducing agent at the entrance of a heat exchanger, so that

it loses its drag reducing properties and therefore regains its heat transfer properties while in the heat exchanger.

This thesis will investigate one of these heat transfer enhancement methods, the use of static mixers. The drag reduction and heat transfer performance of a static mixer design was studied under different flow conditions. The variables considered were fluid temperature, mixer length, fluid composition, and Reynolds numbers along with measurements of the pressure loss penalty caused by the enhancer.

Literature Review

The phenomenon of drag reduction was discovered by Toms[1] and Mysels[2], when they found that adding high polymers and aluminum soaps to flowing fluids could reduce the system pressure loss. Since then research has been conducted to better understand the mechanism of drag reduction, find effective and environmentally benign drag reducing agents, and control the properties of this phenomenon. Some of the potential areas of application include district heating and cooling systems[3], oil pipeline systems[4], sewage systems[5], fire fighting[6], and biomedical systems[7].

To calculate the amount of drag reduction, the Fanning friction factor must first be calculated to estimate the pressure loss of solvent flow using Equation 1:

$$f = \frac{\Delta P D}{2\rho V^2 L} = \frac{\pi^2 D^5 \Delta P}{32 \rho L Q^2}$$

ΔP = pressure drop
D = pipe diameter
ρ = density (1)
V = mean flow velocity
L = pipe length
Q = volumetric flow rate

The percent drag reduction is then defined by Equation 2:

$$\%DR = \frac{f_s - f}{f_s} X 100$$

f_s = solvent friction factor (2)
f = measured solution friction factor

The solvent friction factor is calculated using the von Karman or Prandtl-Karman equation or Equation 3:

$$f^{\frac{-1}{2}} = 4.0 \log(N_{\mathrm{Re}} f^{\frac{1}{2}}) - .4 \quad (3)$$

N_{Re} = Reynolds number

As mentioned before, the two types of drag reducing agents utilized by industry are high polymers and surfactants. Use of polymer additives was the first large scale practical application of drag reduction when they were used in the 800-mile Alyeska crude oil pipeline to increase throughput by up to 25% or 500,000 barrels of crude per day[8]. High polymers are now used extensively by the oil industry in hydrocarbon transport by large corporations such as Shell, Dow Chemical, and ConocoPhillips[9]. Recent research has focused on surfactant drag reducing agents because of their ability to repair their microstructure through self-assembly, which makes them viable in recirculation systems, in which they are subjected to high shear in pumps.

When surfactant solutions reach a special concentration called the critical micelle concentration, the surfactant molecules form spherical micelles. Upon reaching their second critical micelle concentration, these spherical micelles turn into rod-like or thread-like micelles[10]. It is this micellar structure that mechanically degrades when exposed to high shear stress but is able to repair itself through self-assembly. Though the exact mechanism of surfactant drag reduction is not known, it is generally believed that these rod-like micelles are responsible for the drag reduction phenomenon[10].

There are three mechanisms for surfactant drag reduction that have been presented in literature, and all of them revolve around dampening turbulent eddy currents and cross-directional flow, which in turn dissipates energy loss. The first theory is that the rod-like micelles become entangled and their elastic properties hinder cross-flow[11]. The second theory is that the micellar structure leads to an increased extensional viscosity which is responsible for the dampened eddy effects[12]. The third theory is that the rod-like micelles become elongated in the direction of the flow and lead to a thickening of the

viscous sublayer of flow. This thickened sublayer then opposes the cross-directional flow and eddy currents[13].

One of the other traits of drag reducing solutions is a significant reduction in heat transfer[14]. In fact, it has been shown that the heat transfer reduction is always slightly larger than the accompanying drag reduction[15]. The thickened viscous sublayer mentioned previously is believed to increase the thermal resistance between the fluid and the wall by dampening the cross-flow patterns that are thought to be part of the mechanism for heat transfer[16]. The percentage of heat transfer reduction is defined in Equation 4:

$$\%HTR = \frac{Nu_S - Nu}{Nu_S} X100$$
$$Nu_S = \text{Solvent Nusselt Number} \quad (4)$$
$$Nu = \text{Solution Nusselt Number}$$

The Nusselt number for flow in tubes is defined in Equation 5:

$$Nu = \frac{h_i D_i}{k}$$
$$h_i = \text{inner tube heat transfer coefficient} \quad (5)$$
$$D_i = \text{inner tube diameter}$$
$$k = \text{heat conductivity}$$

This reduction in heat transfer can be a beneficial or detrimental side effect depending on the specific application. When drag reducing agents are utilized in oil pipelines, this is very beneficial because minimal insulation has to be used on the pipelines. The oil is heated so that it becomes less viscous and therefore flows more easily. The more heat energy that is saved, the more efficient the process is. On the other hand, sometimes heat transfer is essential to the functioning of the system, such as in district heating and cooling systems. These are systems that utilize a central location

to heat or cool a primary flow loop of water, which is then pumped to nearby buildings, where it exchanges heat with a secondary flow loop of water. This secondary flow loop is then used to heat or cool the individual building it is housed in. Any reduction in operating or capital costs due to drag reduction would be negated by the larger reduction in heat transfer and the need for larger heat transfer areas. These systems have been widely used in Europe for decades and are growing in popularity in the United States and other areas of the world. One of the main reasons these systems are growing in popularity is that they can use waste heat from electrical power generation plants to heat the primary water used for circulation. They also eliminate the need for individual heating and cooling units in the buildings within the district, which frees up more space in the buildings and reduces overall capital costs and maintenance requirements.

Several different methods of enhancing the heat transfer properties of drag reducing solutions have been researched. The general approach to heat transfer enhancement is to destroy the rod-like micellar structure at the entrance of a heat exchanger so that the micelle structure is broken up and the solution loses its drag reducing properties and therefore regains the heat transfer properties of the solvent as it flows through the heat exchanger. After the solution passes through the heat exchanger, the micellar structure should repair itself through self-assembly and thus regain its drag reducing capability.

Some of the methods are simple and some are more complicated. One method is to place a pump near the entrance of the heat exchanger to create an area of high shear stress to destroy the micellar structure[17]. This solution is not always possible in existing systems and represents a significant design constraint. A second method is to use a fluted

tube-in-tube heat exchanger, which means the exchanger has spiral grooves cut into the walls of the piping[18]. These grooves impart spin and shear stress into the flow, which improve heat transfer ability. These heat exchangers are well suited for newly designed systems. A third method is to sharply increase the fluid flow velocity at the entrance of the heat exchanger by introducing a small diameter pipe[17]. The increased shear stress will break up the micellar structure of the drag reducing solution. A fourth method is to use ultrasonic energy to create cavitation bubbles in the fluid flow[10]. When these cavitation bubbles collapse, they can mechanically degrade the surfactant structure. A final method is to place a destructive device at the entrance of the heat exchanger to mechanically degrade the micellar structure of the drag reducing agent[17]. These devices could be wire meshes, honeycomb structures, or static mixers. These devices are simple, cheap, have no moving parts, and can reasonably be installed into any type of drag reduction system. The drawback, however, is that the pressure drop penalty may be large.

Experimental

The experiments run for this research consisted of running two different types of tests at different system settings. In drag reduction tests, the pressure drop was measured to determine the percent drag reduction. In heat transfer tests, the temperature change across a heat exchanger was measured to determine the inner wall heat transfer coefficient.

The materials used were water, ethylene glycol, tris (2-hydroxyethyl) tallow ammonium acetate (EO12), and sodium salicylate (NaSal). Water was used as the process fluid, the solvent in the drag reducing solution, and as part of the heat transfer fluid. Ethylene glycol was used in a 50/50 mixture with water as the heat transfer fluid in all of the system chillers. EO 12 (5.0 mM) and NaSal (12.25 mM) were mixed with water and served as the drag reducing agent in these experiments.

Table 1 below presents the equipment used in the experimental setup with model numbers and manufacturers.

Table 1: Experimental Equipment Details

Equipment	Model	Manufacturer
Pressure gauges (10)	PX 2300-100I	Omega
Pressure gauge	45055	Trerice
Pressure gauge	9185-04	Trerice
Chiller 1	1160	VWR
Chiller 2	RTE-111	Neslab
Chiller 3	LT-HRE-1650-9650-WC-DI-SS	BayVoltex
Main Loop Magnetic Flowmeter	LF404	Toshiba
Heater	STFT-1500-120	TruHeat
Adjustable Speed Drive	1D15J201-ER	Baldor
Drive Motor (Pump)	10NM3562	Inverter
Remote Thermocouple Connection Module	OMB-POD-1	Omega
Chillers 1 & 2 Positive Displacement Flowmeter	JVM-60KG-75-NPT	AW Company
Chiller 3 Magnetic Flowmeter	FMG-705	Omega-mag
Data Acquisition System	Version 7.15.4	Daqview

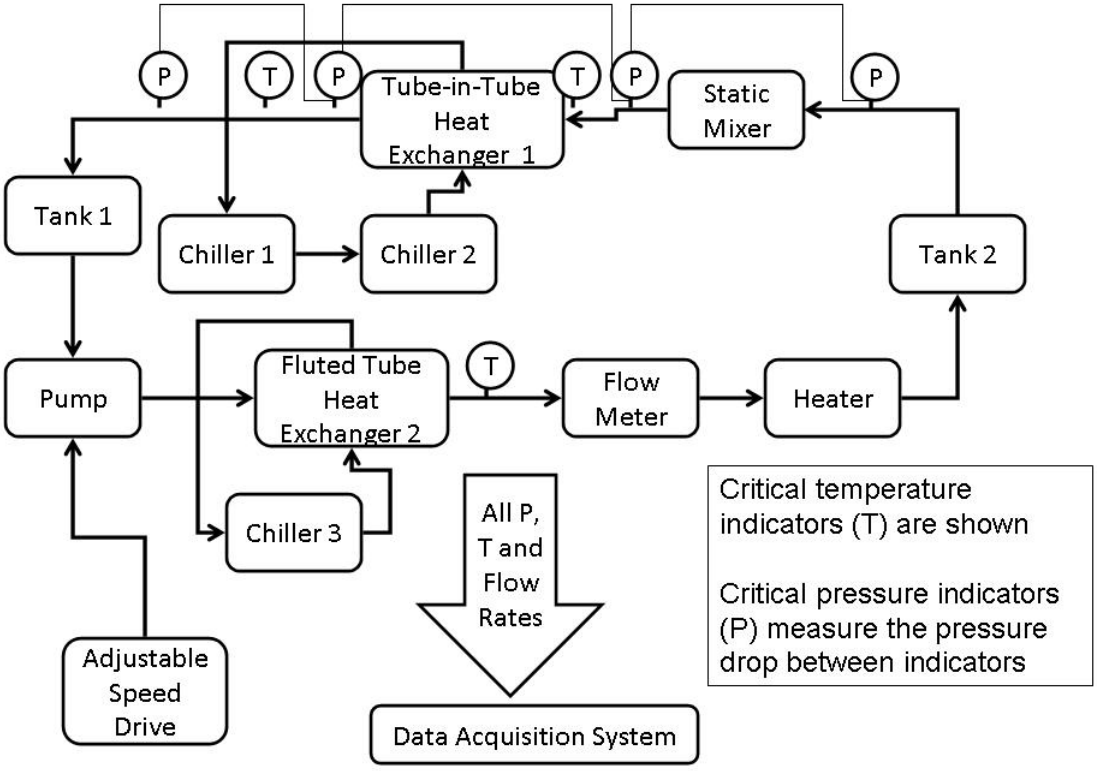

Figure 1: Experimental Setup Flow Sheet

Figure 1 is a schematic flow sheet of the experimental setup. The main flow loop consists of piping connecting tank 1, the pump, heat exchanger 2, the flow meter, the heater, tank 2, the static mixer, heat exchanger 1, and back to tank 1. The two tanks are installed at both ends of the loop to dampen flow fluctuations in order to gather more consistent data. The heater is an electric heater that is used to quickly heat the liquid in the primary loop. Heat exchanger 2 has a fluted inner tube and is used to cool the primary loop through the use of chiller 3. This chiller has a temperature range of -20°C to 10°C and was used to either quickly chill the primary loop or make small adjustments to maintain a steady temperature. The static mixers were placed at the entrance of the heat exchanger in order to destroy the micellar structure of the surfactant drag reducing

solution. Heat exchanger 1 was used as the test heat exchanger. Several thermocouples were placed at the inlet and outlet of both streams entering and exiting the heat exchanger to measure the temperature changes of both the primary fluid and the heat transfer fluid in order to perform heat transfer calculations on the system. The jacket of the heat exchanger was held at a higher temperature than the primary loop and was used to heat the circulating fluid over small temperature intervals. Chillers 1 and 2 were connected in series to provide faster heating and a larger heating capacity. While they are referred to as chillers 1 and 2, they have an effective temperature range of near 0°C to around 100°C and were mostly used to heat the primary loop. There are flow meters connected to each flow loop (primary loop, heat exchanger 1, and heat exchanger 2) in order to measure fluid flow rates for data calculations. There are 10 pressure transducers installed throughout the primary flow loop to measure pressure drop. Each pressure transducer measures the differential pressure drop between two points, so when a transducer is referred to, it is not a single point, but a pipe length of around 30 cm. Figure 2 shows a detailed layout of the pressure transducers. P1 measures the pressure drop across the static mixer section to determine the pressure drop penalty of the mixers tested. P10 measures the pressure drop across heat exchanger 2. P2 measures the pressure drop across heat exchanger 1 and a short distance of piping downstream of it, and the remaining instruments, P3-P9 are placed at equal distances downstream of heat exchanger 1. These remaining eight transducers are used to monitor recovery of drag reduction by the degraded solution in the straight pipe by measuring successive downstream pressure gradients.

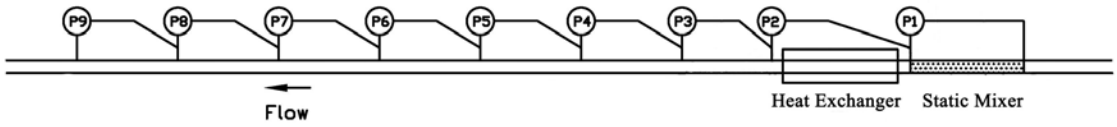

Figure 2: Detailed View of Pressure Transducer Placement

There are also 11 thermocouples installed throughout the system. For example, the most important ones are at the entrance and exit for both fluid flows in heat exchanger 1. Others are placed throughout the primary loop to determine the bulk fluid temperature and also the temperature change across heat exchanger 2. The pump performance was controlled by an adjustable speed drive that was able to control the pump from 0-1,696 RPM. All of the data collected from the various flow meters, pressure transducers, and thermocouples was collected by the data acquisition system and automatically recorded in an Excel spreadsheet.

Table 2 shows the 36 different system settings at which the experiments were run.

Table 2: System Configurations for Experiments

Experiment Number	Type of Experiment (Drag Reduction or Heat Transfer)	Primary Fluid	Static Mixer Length (0, 1, 3 lengths)	Main Loop Temperatures (°C)	Δ T (°C)
1	DR	Water	0	10, 20 & 30	50
2	DR	Water	1	10, 20 & 30	50
3	DR	Water	3	10, 20 & 30	50
4	DR	DR Solution	0	10, 20 & 30	50
5	DR	DR Solution	1	10, 20 & 30	50
6	DR	DR Solution	3	10, 20 & 30	50
7	HT	Water	0	10, 20 & 30	50
8	HT	Water	1	10, 20 & 30	50
9	HT	Water	3	10, 20 & 30	50
10	HT	DR Solution	0	10, 20 & 30	50
11	HT	DR Solution	1	10, 20 & 30	50
12	HT	DR Solution	3	10, 20 & 30	50

The two types of tests run were drag reduction and heat transfer. The two different primary fluids used were water and the surfactant drag reducing solution that consisted of water, EO 12 (5.0 mM), and NaSal (12.5 mM). The three different static mixer lengths were zero lengths (no mixer), one mixer length, or three mixer lengths. Figure 3 below shows what two static mixer lengths look like. It is simply a plastic mixer with a helical shape.

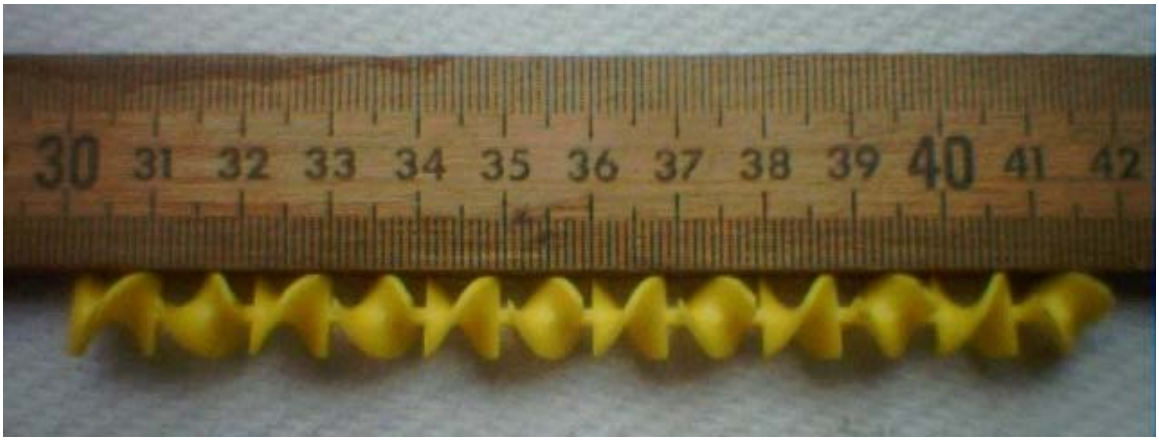

Figure 3: Two Static Mixer Lengths

Each set of system settings was run at 10°C, 20°C, and 30°C. All experiments were run with a ΔT of 50°C for consistency. This is the temperature different between the primary fluid and the heat transfer fluid in heat exchanger 1, which was always 50°C higher.

Half of the tests were run with water as the primary fluid in order to provide baseline data for both drag reduction and heat transfer comparisons at the three different temperatures and static mixer lengths. Once these tests had been run, the water was replaced by the surfactant drag reducing solution in order to measure the percent drag reduction and decrease in heat transfer. Finally, the static mixers were incorporated into

the drag reduction system to see how their presence and length affected the drag reduction and heat transfer properties of the fluid.

To begin a test run, the computer must be turned on with an Excel spreadsheet data template open. Each of the 12 tabs in the spreadsheet represented a different pump flow rate for the given system configuration and temperature. The pump speeds were 114, 143, 201, 258, 316, 517, 718, 919, 1121, 1322, 1523, and 1696 RPM. For drag reduction tests, the next step is to use either chiller 3 or the electric heater to get the primary loop to the desired temperature. When the proper temperature is reached, the next step is to click the data collection button in Excel. This would tell the data acquisition board to run 1000 scans in the next 12 seconds on all of the instruments, output the data to Excel, and then calculate the time averaged values which would be used in calculations. Once this was done, the pump was adjusted to a different speed, and the system was allowed to run for a minute or so to reach a new steady state. At this point, if the temperature was still in the allowable bounds (± 0.5°C), the next data slice would be taken. If the temperature had deviated too far, chiller 3 or the electric heater would be used to bring the temperature back to the acceptable range and then the data slice would be taken. This process continued until data at all 12 flow rates had been collected.

The procedure for a heat transfer test was more complicated. Before the test begins, a small static mixer must be placed slightly downstream of the heat exchanger. It is important to note that this is a different location and design of static mixer than the ones being investigated in these experiments. This is a smaller static mixer that is meant to produce a flat temperature profile slightly downstream of heat exchanger 1. When

fluids pass through a pipe with heated walls, as the primary fluid does in heat exchanger 1, the fluid temperature at the walls is higher than it is in the center of the fluid flow. This results in a curved temperature profile across the fluid flow. The thermocouples in this system are positioned so that they measure the temperature in the center of the flowing fluid, which leads to biased temperatures, especially at the thermocouple nearest to the exit of heat exchanger 1. By installing the static mixer, the primary fluid is mixed, producing a flat temperature profile, so that the thermocouple provides an accurate reading of the mean temperature.

The next step in a heat transfer test is to heat chillers 1 and 2 up to 55°C above the desired primary fluid temperature, while the primary loop is not running. Careful attention must be paid to the holding tanks in chillers 1 and 2. They are two different models connected in series, so often their flow rates are different, which causes the liquid level to increase or decrease in the holding tanks. One of the chillers often needs to be turned off in order to prevent the other from overflowing or being completely empty, which is not good for the pump. Once the desired temperature is reached, chillers 1 and 2 are shut off, and the primary loop is turned on. Chiller 1 or the electric heater is then used to get the primary loop to its desired temperature. When this temperature is reached, chillers 1 and 2 should have cooled down enough to provide a ΔT of 50°C. Thereafter, a combination of chillers 1, 2, 3 and the electric heater were used to maintain the primary loop temperature in the desired range, while also keeping a ΔT of 50°C. This is the most difficult part of the experiment as it requires patience and a thorough working knowledge of the speed and magnitude to which the system will respond to changes in the heating/cooling sources. Once both temperatures are within the acceptable range, the

data collection button is clicked and a 12 second data slice is collected. Then the pump flow rate is changed and the system is allowed to equilibrate again before the process of temperature control and data collection starts again.

There were some problems in the experiments that should be noted. When three static mixer lengths were installed in the system, the maximum pump setting of 1696 RPM could not be reached because the pressure buildup was too high in the system. Also, data could not be taken at some of the lowest flow rates when the primary loop was set to 10°C because the system could not be held at a reliable steady state. The final drawback to the experimental setup was not being able to run tests where the primary loop was at a higher temperature than the heat exchanger fluid in heat exchanger 1. An example of this would be running the primary loop at 80°C while the heat transfer fluid in heat exchanger 1 would be at 30°C, and the primary loop would be acting as a heat source. These tests could not be run because the electric heater was not reliable enough to keep the system at a steady state. Finally, P5 consistently showed erratic behavior when compared to other pressure transducers under the same conditions. The cause of this is unknown, but calibration error or equipment malfunction are the most likely sources. Because of this, the P5 data were not used for data analysis.

Data Reduction

The first step in the data reduction for drag reduction tests was to prepare a friction factor versus Reynolds number graph. The friction factor was calculated using Equation 1, which is shown again below.

$$f = \frac{\Delta P D}{2\rho V^2 L} = \frac{\pi^2 D^5 \Delta P}{32 \rho L Q^2}$$

ΔP = pressure drop
D = pipe diameter
ρ = density (1)
V = mean flow velocity
L = pipe length
Q = volumetric flow rate

The pipe diameter was .0102 meters. The pressure transducer readings were recorded in Volts and then converted to usable units by a calibration equation. The density of water was taken from tabulated values, and the concentration of the drag reducing agents is low enough that the density of water was used for the solution as well. The volumetric flow rate signal was read from the main loop flow meter and then converted to usable units by a calibration equation. Instead of directly using the pipe length, the ratio of L/D was used in equations. This value was determined by the distance between the two points between which the pressure differential was measured. The value for P1 was 50, while P2 was 180. P3-P9 each had a value of 80, and P10 had a value of 100. Friction factors measured at each location were plotted against the solvent Reynolds number. Figures 4 through 6 below show the graphs generated with water as the primary fluid with no mixers at 20°C.

The data series for P1-P10 represent measurements at the 10 different pressure transducer locations in the system. P1 is the pressure drop across the section of piping

where the static mixers are installed. P10 is the pressure drop across heat exchanger 2. P2 is the pressure drop across and directly after heat exchanger 1, and the rest of the transducers are at locations downstream of P2 one after the other. The three lines present on the graphs are models for friction factors. The top line is the von Karman line, which models the friction factor of water and is defined in Equation 3. The fact that most of the data points lie on or near the von Karman line is a sign that the pressure drop data are accurate. The other two lines are maximum drag reduction asymptotes. The middle line is the Virk equation, which represents the minimum friction factors for high polymers and is defined by Equation 6[19].

$$f = .58 N_{\mathrm{Re}}^{-.58} \tag{6}$$

The lowest line is the Zakin-Myska-Chara line, which represents the minimum friction factors for surfactants, and it is defined by Equation 7[19].

$$f = .32 N_{\mathrm{Re}}^{-.55} \tag{7}$$

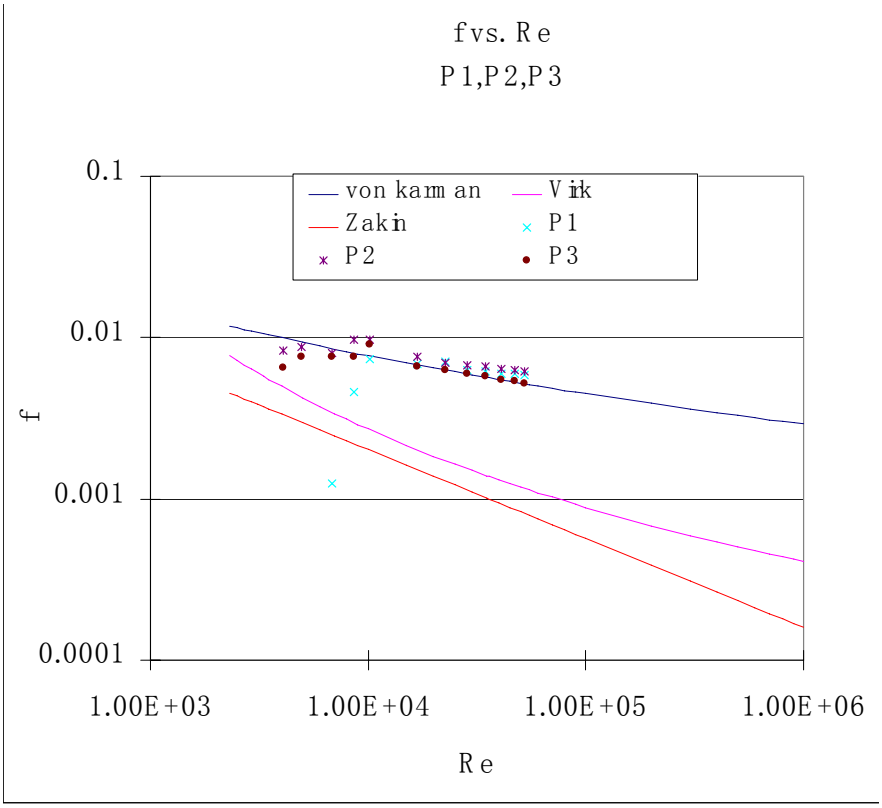

Figure 4: Friction Factor Measured at P1, P2, & P3 vs. Reynolds Number for Water with No Mixer at 20°C

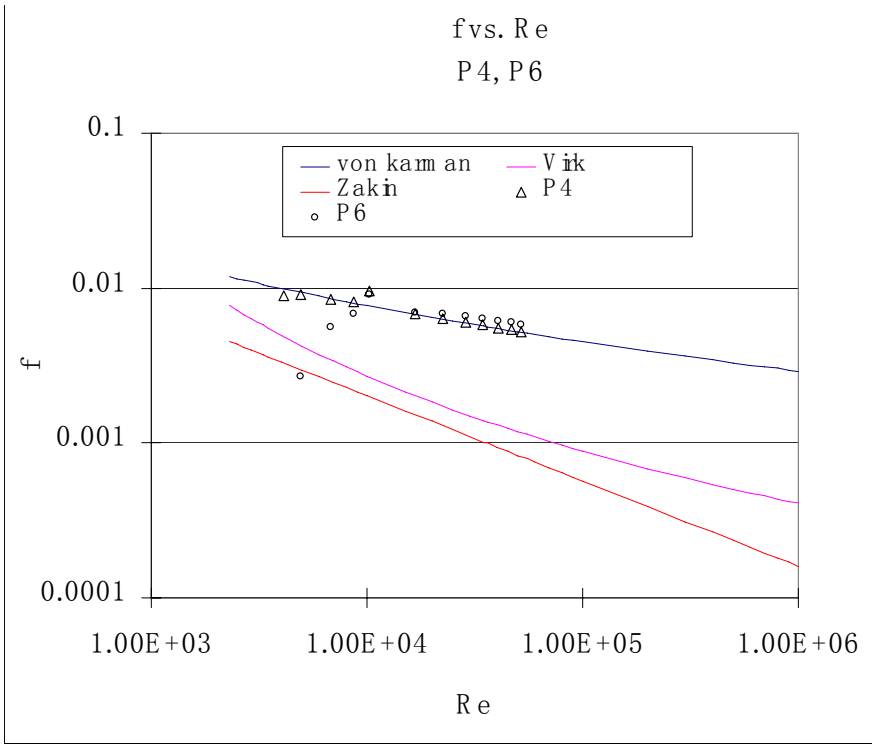

Figure 5: Friction Factor Measured at P4 & P6 vs. Reynolds Number for Water with No Mixer at 20°C

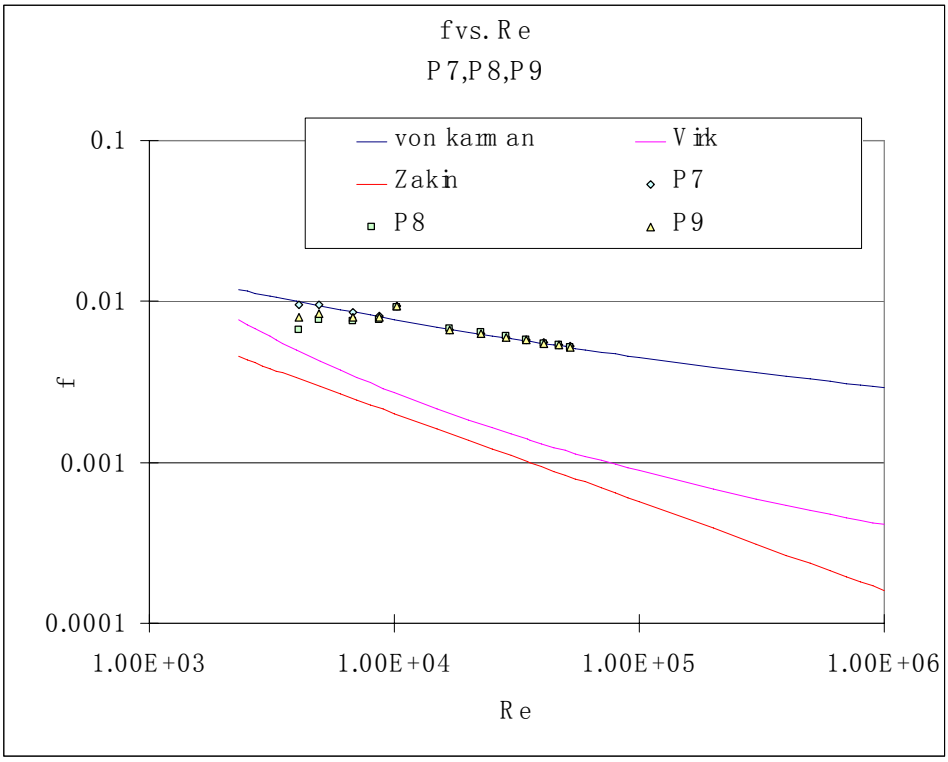

Figure 6: Friction Factor Measured at P7, P8, & P9 vs. Reynolds Number for Water with No Mixer at 20°C

Figures 7 to 9 show the graphs generated when the drag reducing solution was used with no mixer at 10°C.

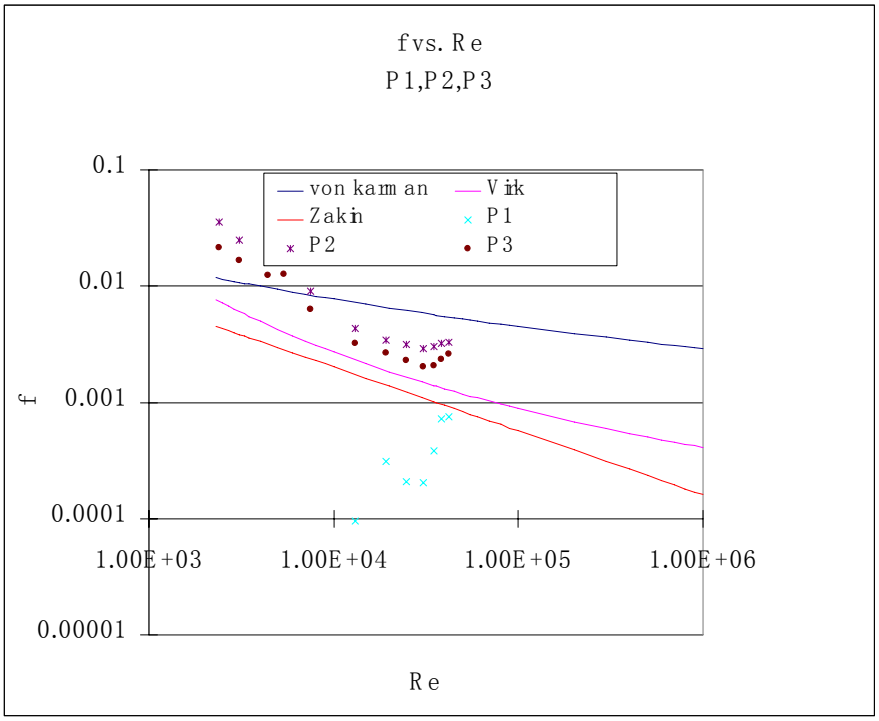

Figure 7: Friction Factor Measured at P1, P2, & P3 vs. Reynolds Number for Drag Reducing Solution with No Mixer at 10°C

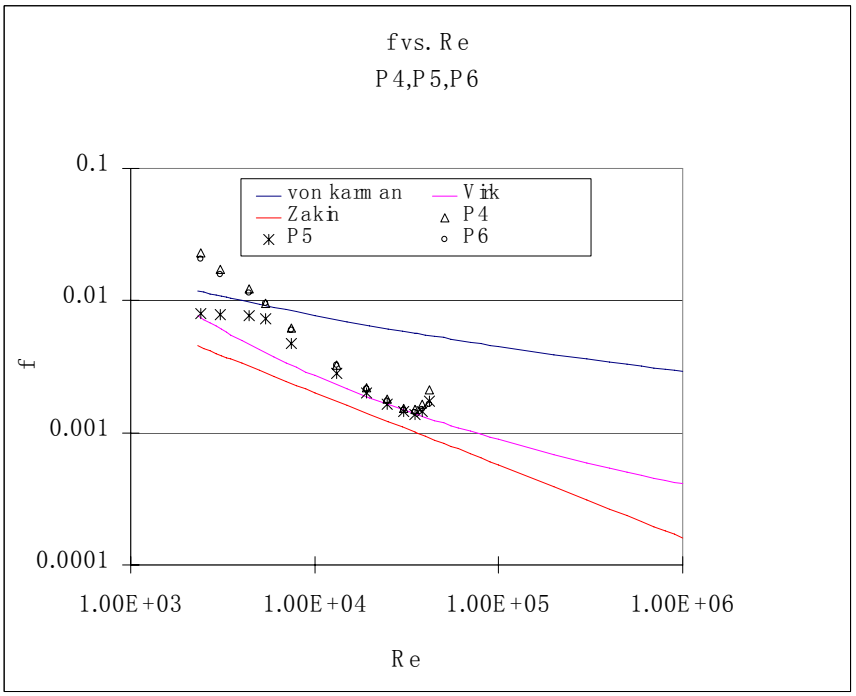

Figure 8: Friction Factor Measurement at P4, P5, & P6 vs. Reynolds Number for Drag Reducing Solution with No Mixer at 10°C

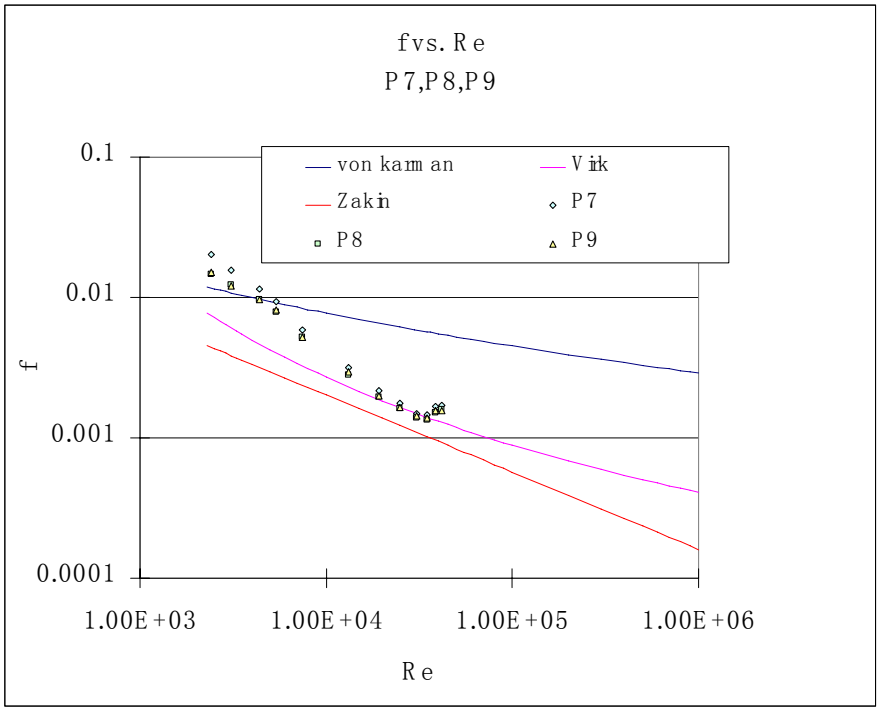

Figure 9: Friction Factor Measured at P7, P8, & P9 vs. Reynolds Number for Drag Reducing Solution with No Mixer at 10°C

In these graphs, the friction factors fall well below the von Karman line but do not reach the Zakin-Myska-Chara line which represents the minimum attainable friction factors. The piping section that P1 covers has two crimps in it to hold static mixer lengths in place, which alters the pressure drop giving different friction factors as well.

The next step in the data analysis is to plot the percent drag reduction against the Reynolds number. This is calculated using Equation 2. Figures 10 and 11 below show the percent drag reduction plots from the two system settings mentioned previously in this section. As expected, the water shows no drag reduction in the region where turbulent flow is fully developed, while the surfactant solution shows a significant amount.

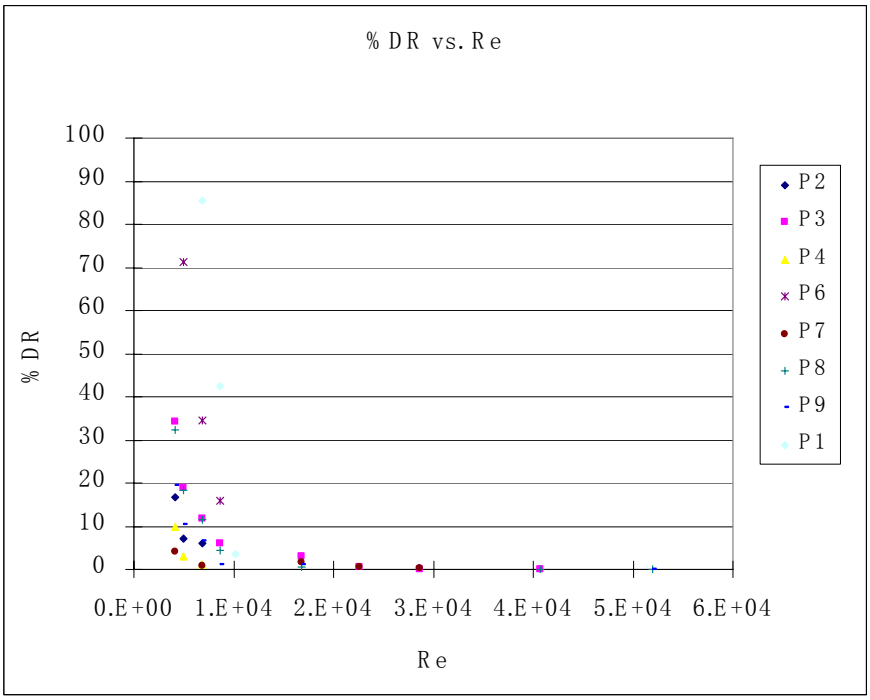

Figure 10: Percent Drag Reduction vs. Reynolds Number for Water with No Mixer at 20°C

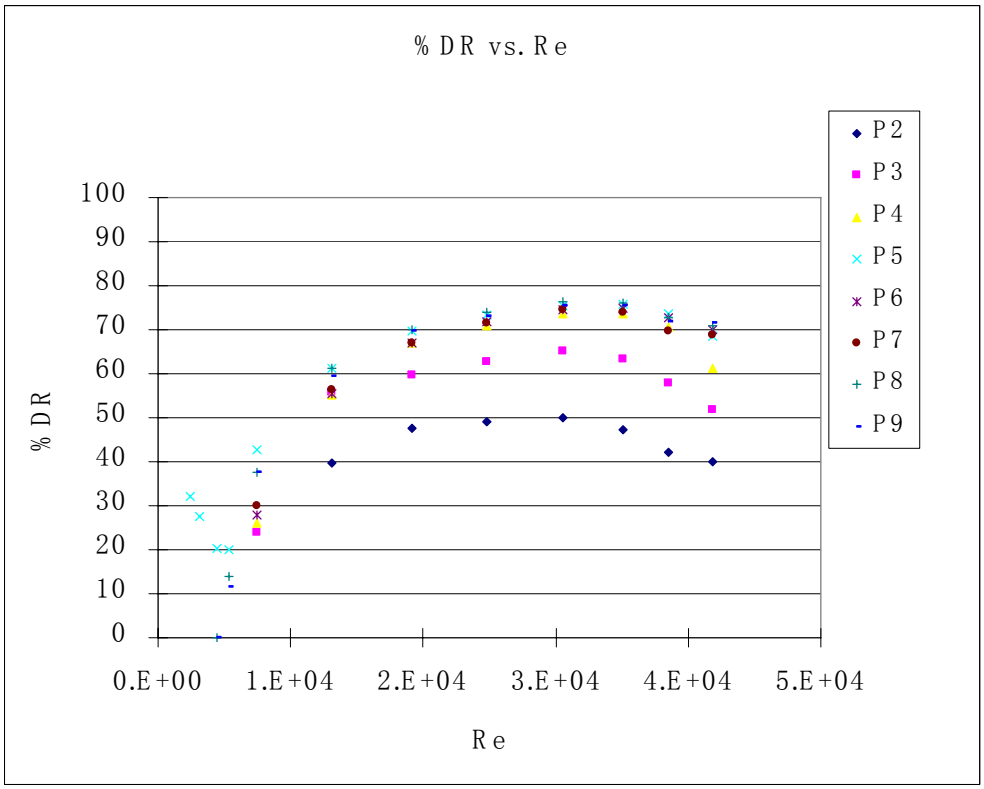

Figure 11: Percent Drag Reduction vs. Reynolds Number for Drag Reducing Solution with No Mixer at 10°C

These drag reduction graphs were also used to calculate the recovery time of the surfactant solution. This is the time it takes the solution to regain its drag reducing properties after going through a region of high sheer. At each Reynolds number, the least downstream transducer to show fully drag reduction properties was used to calculate the recovery time. For example, in Figure 11 at a Reynolds number of approximately 30,000, there is a tight cluster of data points around 75% drag reduction. This was assumed to be the maximum percent drag reduction at those system conditions. The figure shows that P2 and P3 do not show full drag reduction behavior, so the start of P4 would be chosen as the recovery point for the surfactant solution. The recovery time was then calculated by dividing the distance from the end of the static mixer to the recovery point by the fluid velocity. The recovery points can vary for each Reynolds number, however. For example, Figure 11 shows that at an approximate Reynolds number of 40,000, P4 does not show full drag reduction behavior, so its recovery point is at P5.

The data reduction for the heat transfer experiments was more complicated and was based largely on previous work done by this research group[19]. The final goal is to calculate the inner wall heat transfer coefficient. The process is slightly different for water and drag reducing solution test runs, so the process for water experiments will be discussed first. The first step is to compare the two separate heat balances to verify that the data are reasonably accurate. Equation 8 below shows the equation used to calculate the heat balances.

$$Q = V\rho Cp\Delta T$$

Q = amount of heat transferred
V = volumetric flow rate
ρ = density
Cp = heat capacity
ΔT = temperature change

(8)

This calculation is done on the annulus side as well as the primary loop of heat exchanger 1. Ideally the values from each calculation should be equal, but this was not generally the case. Figure 12 below shows a plot of the heat balances with typical deviations. This plot shows data from a test using water as the primary fluid with 3 static mixer lengths at 30°C. When running experiments, if there was a large heat unbalance, the tests were repeated in order to acquire data that were in better agreement.

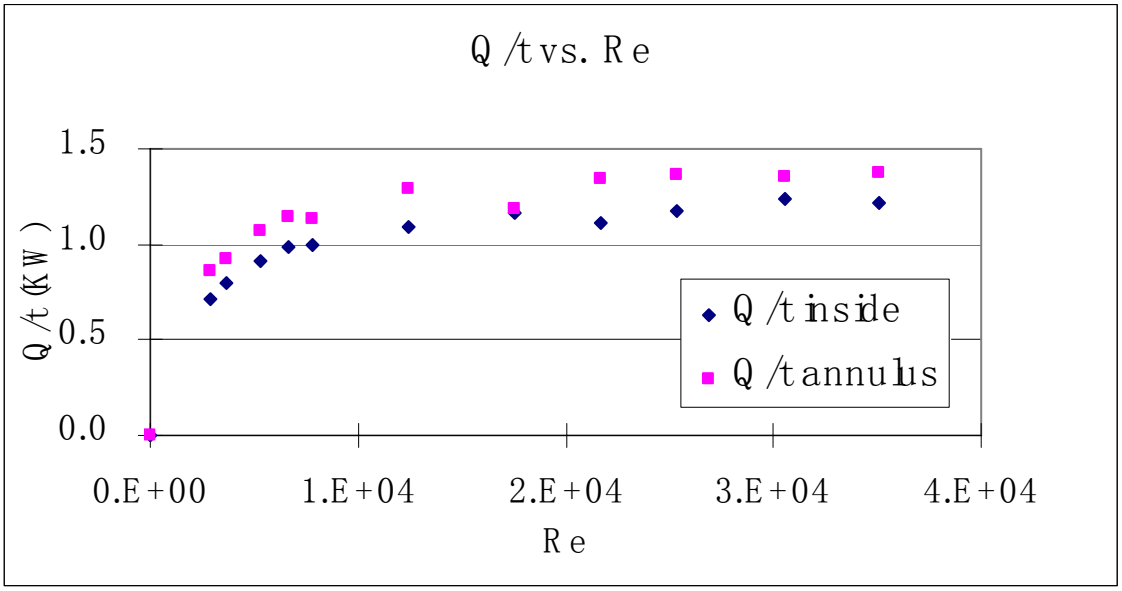

Figure 12: Heat Balance Plot for a Water System with 3 Static Mixer Lengths at 30°C

The next step was to calculate the inner wall heat transfer coefficient through the modified Wilson plot method. The total thermal resistance is made up of the inner and outer boundary resistances and the wall resistance as shown in Equation 9.

$$R_{Tot} = R_i + R_w + R_o = \frac{1}{A_i h_i} + R_w + \frac{1}{A_o h_o} = \frac{1}{A_i C_i F} + R_w + \frac{1}{A_o C_o G}$$

A_i = inner wall area

A_o = outer wall area

C_i = inner wall constant (9)

C_o = outer wall constant

F = inner wall empirical factor

G = outer wall empirical factor

The total resistance and wall resistance can be determined from experimental data using Equations 10 and 11.

$$R_{Tot} = \frac{1}{UA} = \frac{\Delta T_{lm}}{\dot{m} C_p \Delta T}$$

U = overall heat transfer coefficient

A = heat transfer area (10)

ΔT_{lm} = log mean temperature difference

$\dot{m}$ = mass flow rate

$$R_w = \frac{(D_o - D_i)}{2 k_B \pi D_{lm} L}$$

D_o = outer wall diameter

D_i = inner wall diameter (11)

D_{lm} = log mean diameter

k_B = heat conductivity of wall

L = heat exchanger length

The next step is to plot Equation 12, which allows the variables C_i and C_o to be found from linear regression analysis[19]. This entails plotting $(R_{Tot} - R_w)GA_o$ against $\frac{GA_o}{A_i F_i}$. This data should show a linear relationship where C_i is the inverse of the slope, and C_o is the inverse of the y-intercept. The variables F and G are parameters derived empirically in other research studies that are used to calculate heat transfer coefficients and are defined by Equations 13[19] and 14. C_i and C_o are constants created for this

method as well . Equation 14 differs from that used previously in the research group because of a different experimental setup. Previously a steam heated heat exchanger had been used, which required a different equation. Equation 14 better models a tube-in-tube heat exchanger that utilizes a heat transfer liquid[20].

$$(R_{Tot} - R_w)GA_o = \frac{GA_o}{A_i F C_i} + \frac{1}{C_o}$$

A_i = inner wall area (12)

A_o = outer wall area

$$F = \frac{\frac{f}{8}(\mathrm{Re}_{Water} - 1000)\,\mathrm{Pr}_{Water}}{(1 + 12.7(\frac{f}{8})^{.5}(\mathrm{Pr}^{2/3}_{Water} - 1))}\left[1 + \left(\frac{D_i}{L}\right)^{\frac{2}{3}}\right]\left(\frac{\mathrm{Pr}_{Water}}{\mathrm{Pr}_{Water-Twall}}\right)^{.11}\left(\frac{k_{Water}}{D_i}\right) \quad (13)$$

Pr = Prandtl number

$$G = .023\left(\frac{\dot{m}\Delta D}{\mu_F}\right)^{.8}\left(\frac{\upsilon}{\alpha}\right)^{1/3}\left(\frac{\Delta D}{D_o}\right)^{.45}\left(\frac{k}{\Delta D}\right)$$

ΔD = diameter difference

μ_F = viscosity at film temperature (14)

υ = kinematic viscosity

α = thermal diffusivity

The inner wall heat transfer coefficient can be found by taking part of Equation 9 and rearranging it to create Equation 15 and can be plotted against Reynolds number as shown in Figure 13.

$$h_i = \frac{F}{C_i} \quad (15)$$

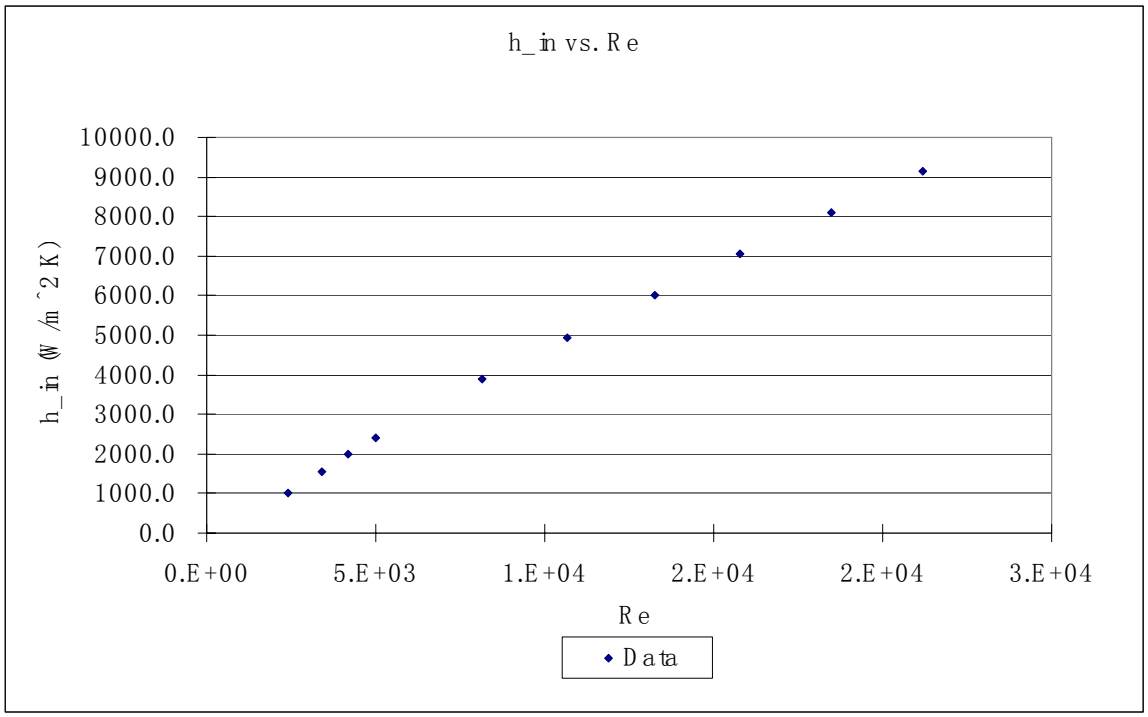

Figure 13: Plot of Inner Wall Heat Transfer Coefficient vs. Reynolds Number for Water with 3 Static Mixer Lengths at 10°C

Finally, the Nusselt number can be calculated using Equation 5 and can be plotted against Reynolds number as shown in Figure 14.

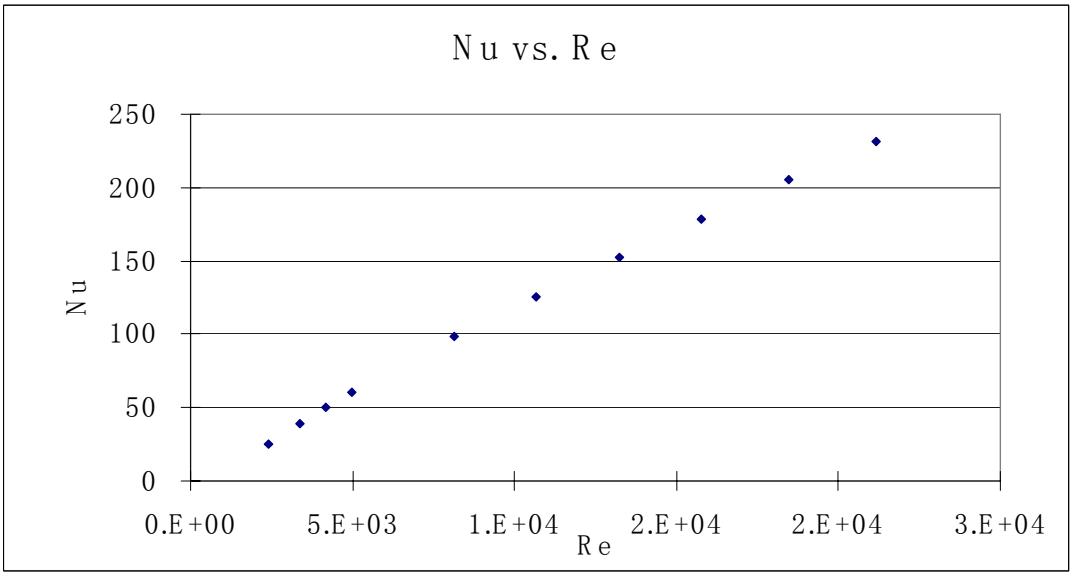

Figure 14: Plot of Nusselt Numbers vs. Reynolds Number for Water with 3 Static Mixer Lengths at 10°C

The process for surfactant drag reducing solution systems is different because there is no reliable equation for F for surfactant solutions in this type of system. Because the heat transfer fluid in the annulus is the same in both experiments, it was assumed that G and C_o calculated for water tests at the same temperature are valid for the solution tests as well. Using this assumption, the inner wall heat transfer coefficient can be calculated for the surfactant systems using Equation 16. That is, the total resistance is calculated using the surfactant data, while G and C_o are calculated using data from water tests under the same conditions. The Nusselt number can then be calculated in the same fashion as water tests.

$$h_{i,surf} = \frac{1}{(R_{tot,surf} - R_W - \frac{1}{C_{o,water} A_o G_{water}})A_i} \tag{16}$$

Results and Discussion

The first task in dealing with the results was to verify that the experimental setup produced reasonably accurate data. The two ways that this was accomplished was by comparing the pressure drop data for water to the von Karman line and to compare heat balances for the primary flow loop to that of the annulus in heat transfer tests.

Figures 4 to 6 are redisplayed below for clarity.

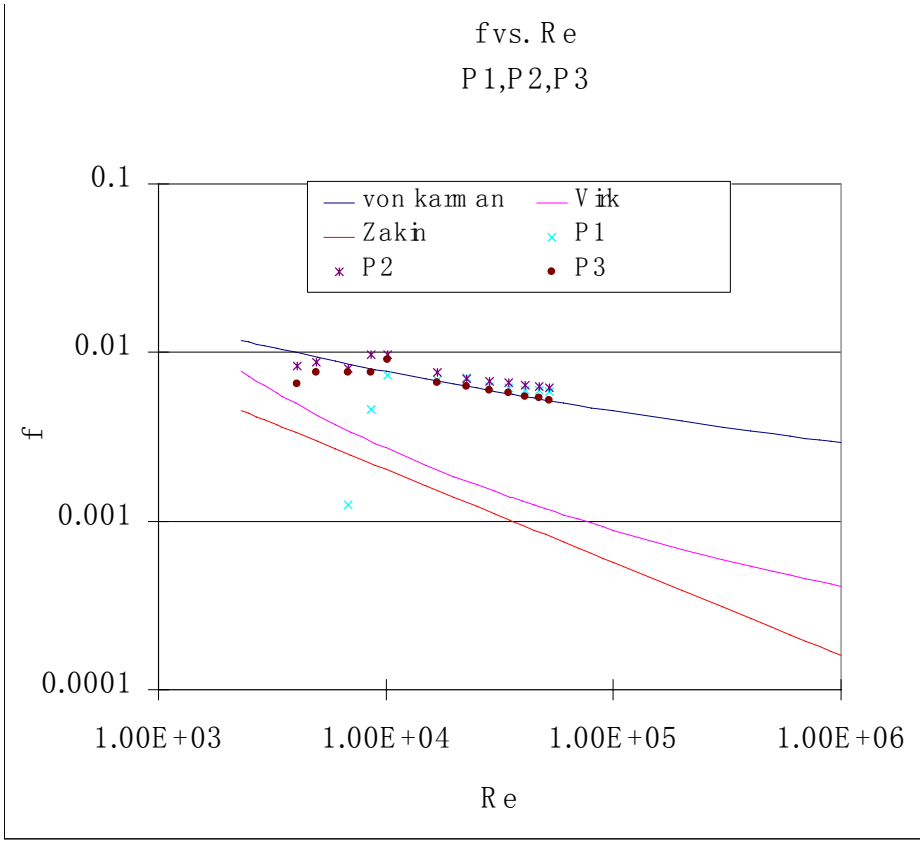

Figure 4: Friction Factor Measurement at P1, P2, & P3 vs. Reynolds Number for Water with No Mixer at 20°C

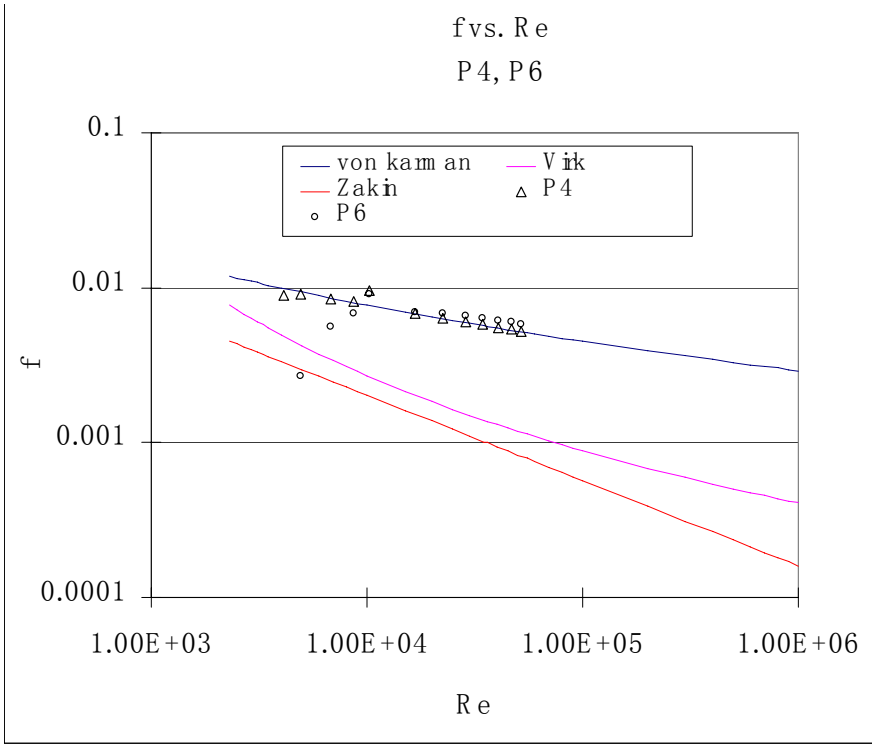

Figure 5: Friction Factor Measurement at P4 & P6 vs. Reynolds Number for Water with No Mixer at 20°C

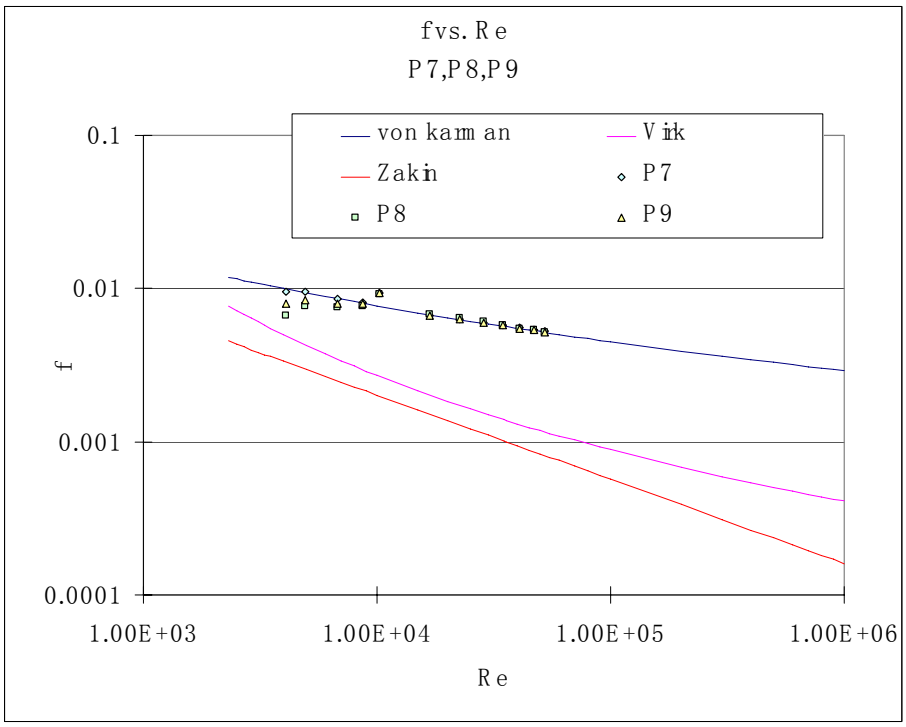

Figure 6: Friction Factor Measurement at P7, P8, P9 vs. Reynolds Number for Water with No Mixer at 20°C

These three plots are good representations of the behavior of the friction factor versus Reynolds number plots for water systems. Because there are no mixers in this test, it also represents the most basic pressure drop data for this experimental setup. The data agree to within 3% of the von Karman line on P3, P4, P7, P8, and P9 when the Reynolds number is above 10,000, where turbulent flow is fully developed. While some of the other data deviate more, most of this can be explained by experimental conditions. The data points below Reynolds numbers of 10,000 are not very accurate because turbulent flow is not fully developed, which explains the deviation from the von Karman line. Also, P1, P2, and P10 do not measure the pressure drop over smooth pipe segments, which alters their pressure drop measurements. P1 and P2 both have crimps in them to hold static mixer lengths in place, and P10 measures the pressure drop across a fluted length of pipe. As explained earlier, P5 produced erratic data throughout the entire testing process. Since these factors explain much of the deviation, it appears that the pressure transducers collect reliable and accurate data at P3, P4, and P6-P10.

To check the accuracy of temperature measurements, the amount of heat transferred was computed for the annulus and the primary loop. Ideally, these two values would be the same, but this was often not the case. Figures 15 and 16 show good and bad agreement. Figure 15 shows excellent heat balance agreement for the water test with no mixer at 30°C. The maximum deviation is 10%, but most fall under 5%. Figure 16, however, shows a test with poor agreement for water with three static mixers at 20°C, where all data points deviate by at least 10%. The reason for this variance between tests is most likely instrument error. The thermocouples and flow meters were in sync for

some tests but not for others. When tests with poor heat balance agreement were obtained, the heat balance measurements were repeated until better results were achieved.

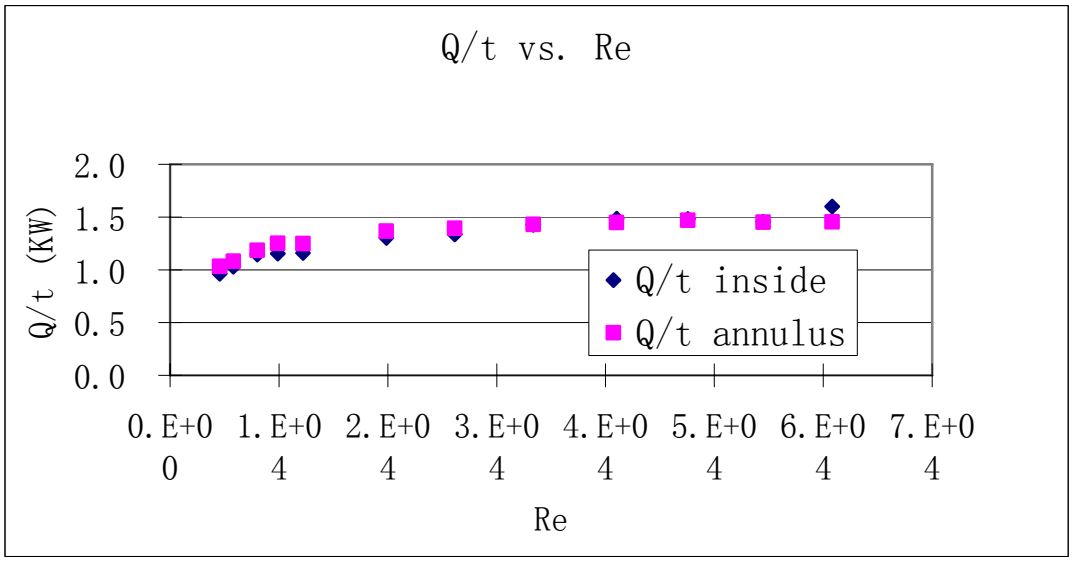

Figure 15: Heat Balance Plot for Water Test with No Mixer at 30°C

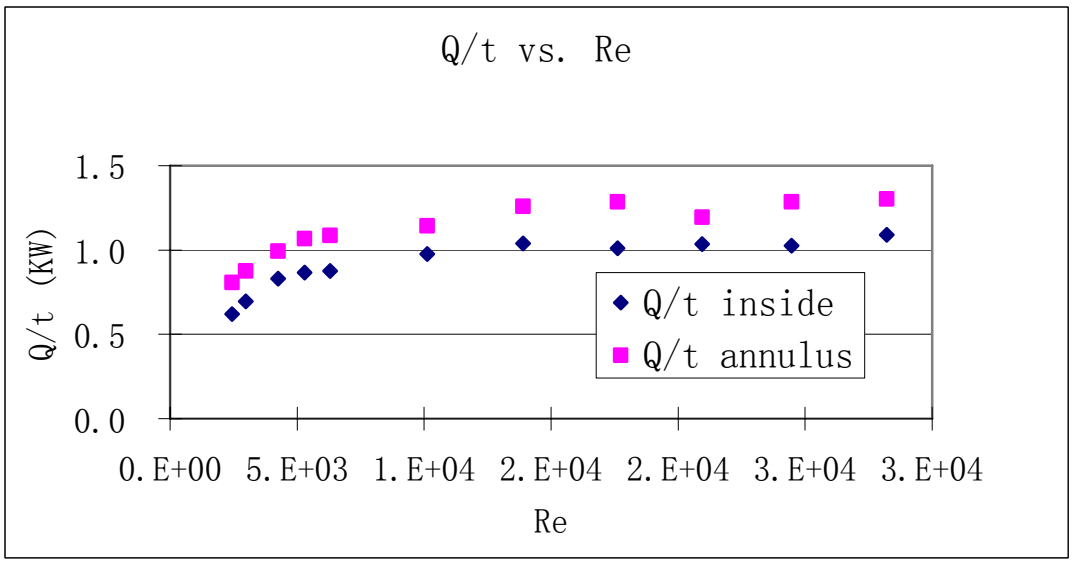

Figure 16: Heat Balance Plot for Water Test with Three Static Mixer Lengths at 20°C

The second step to verifying accurate temperature readings was to compare the measured heat transfer coefficient to a published correlation for turbulent flow in a pipe. The correlation used is shown in Equation 17[21]. The comparison between the correlation

results and the measured data is shown in Figure 17. There is good agreement between the two sets of data, with an average error of 15%. The average deviation is less than under 8%, however, for Reynolds numbers above 10,000. This is the range for which Equation 17 is reliable[21].

$$Nu = .023 * \mathrm{Re}^{.8} * \mathrm{Pr}^{.4}$$
$$Nu = \text{Nusselt number}$$
$$\mathrm{Re} = \text{Reynolds number} \qquad (17)$$
$$\mathrm{Pr} = \text{Prandtl number}$$

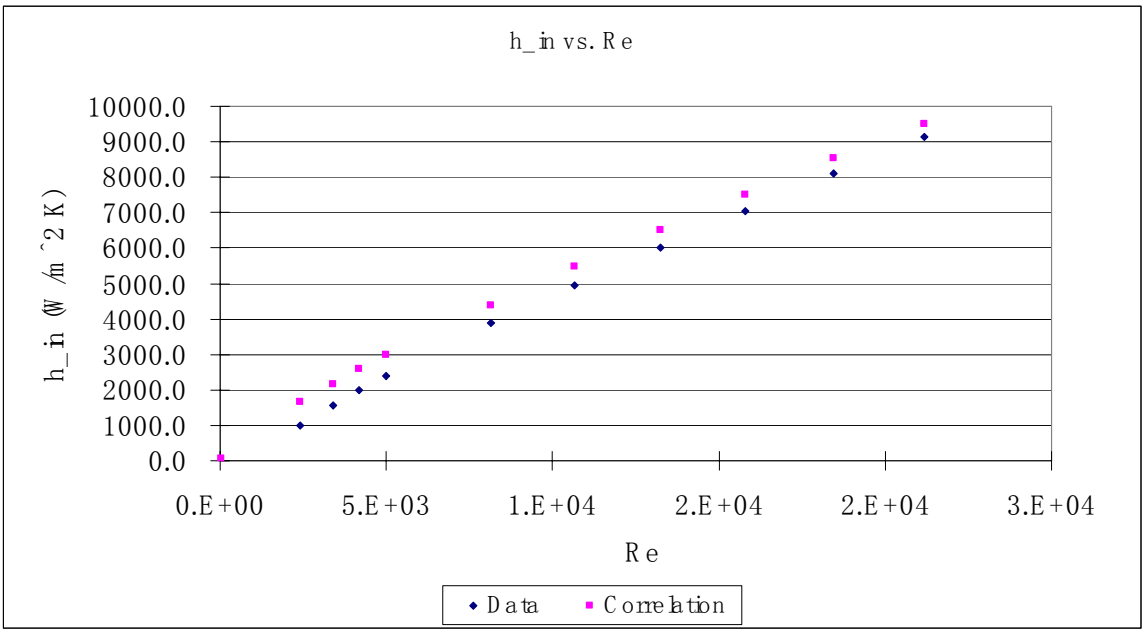

Figure 17: Heat Transfer Coefficients vs. Reynolds Number for Water Test with Three Static Mixer Lengths at 10°C

It was also necessary to establish that the surfactant system was an effective drag reducing agent. This is done by comparing the percent drag reduction of the solution to water at the same temperature. Figures 18 and 19 compare water and the drag reducing solution at 10°C. Figures 20 and 21 compare the two fluids at 20°C, and Figures 22 and 23 compare them at 30°C

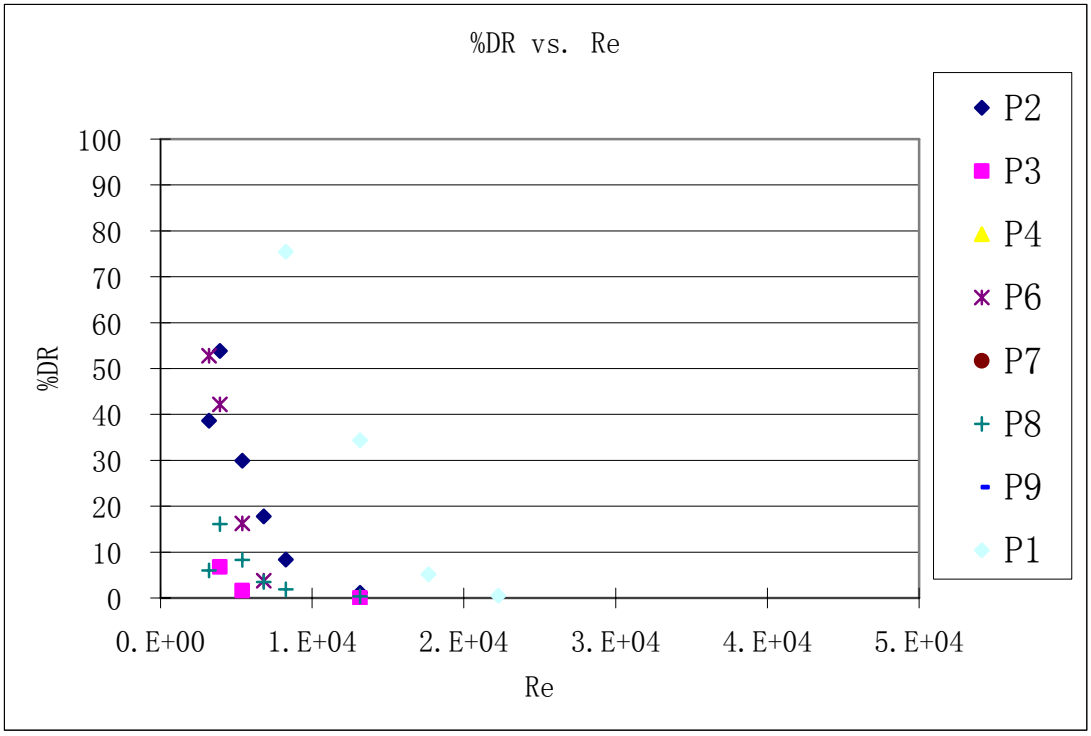

Figure 18: Percent Drag Reduction Plot for Water Test with No Mixer at 10°C

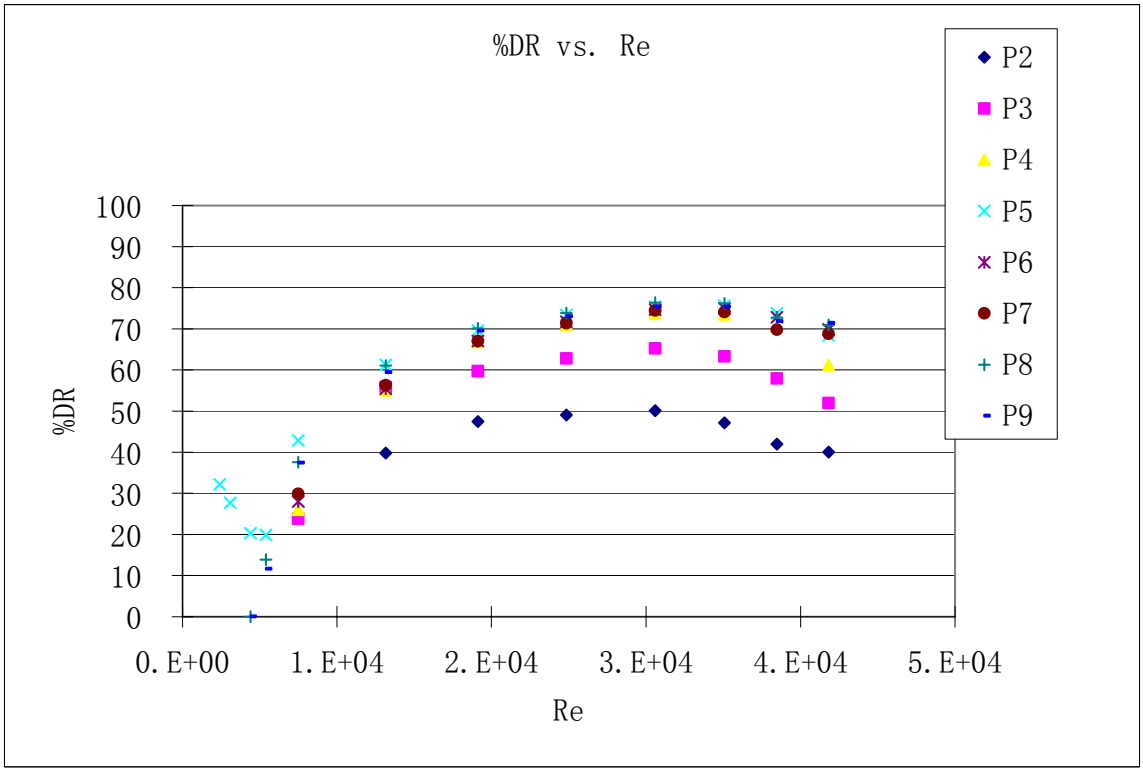

Figure 19: Percent Drag Reduction Plot for Drag Reducing Solution Test with No Mixer at 10°C

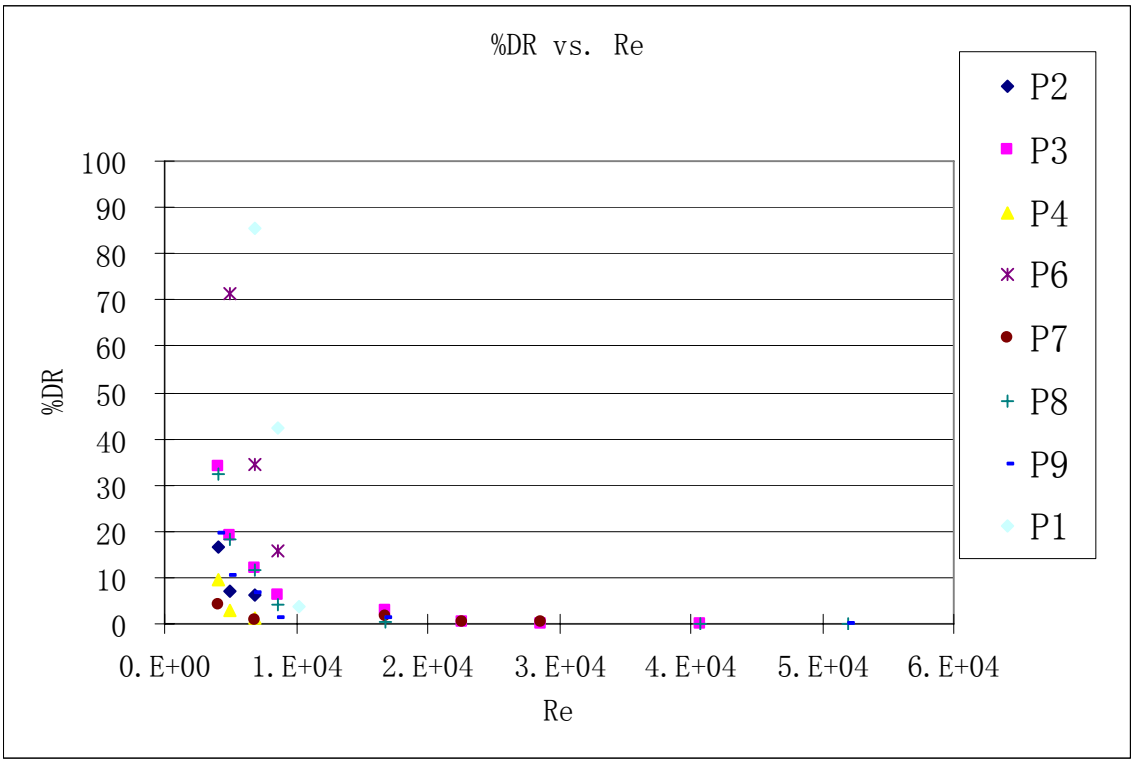

Figure 20: Percent Drag Reduction Plot for Water Test with No Mixer at 20°C

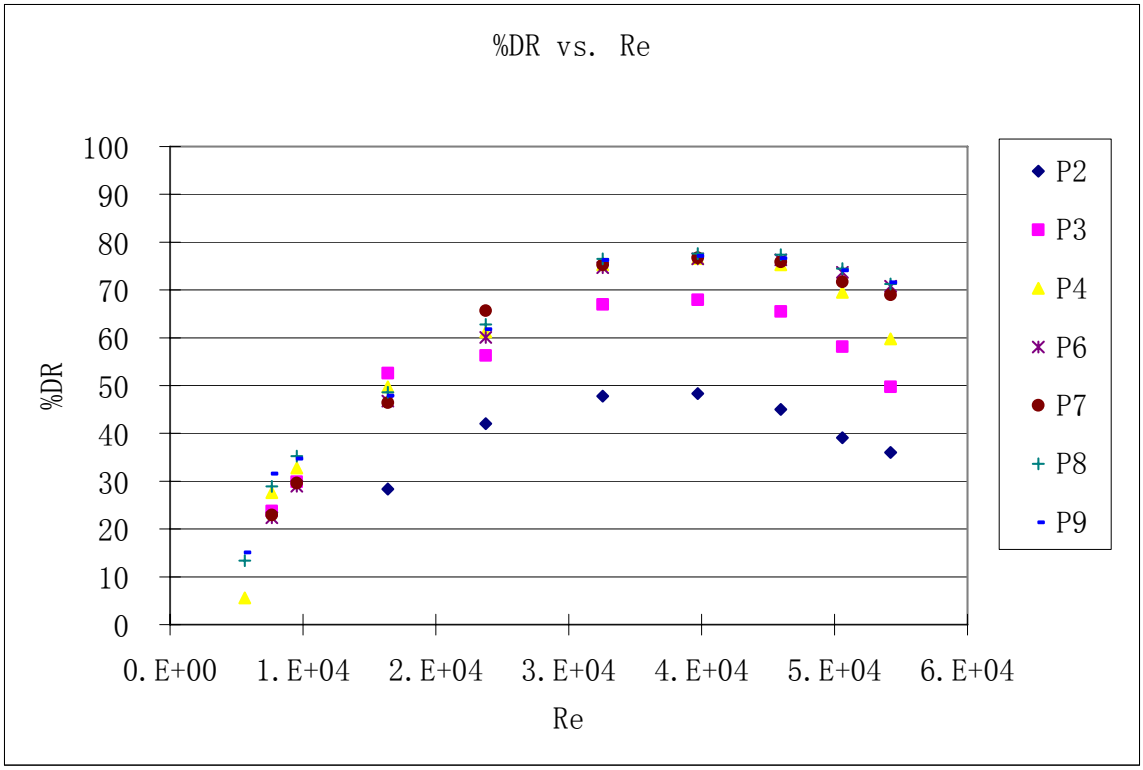

Figure 21: Percent Drag Reduction Plot for Drag Reducing Solution Test with No Mixer at 20°C

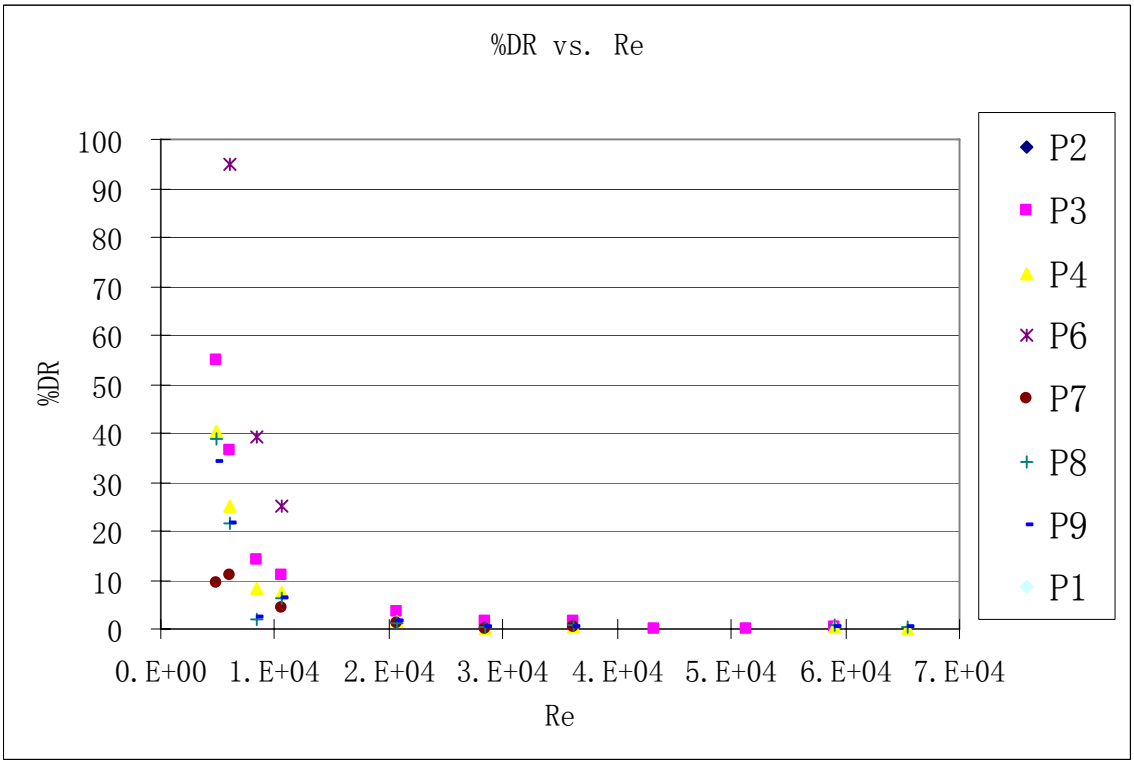

Figure 22: Percent Drag Reduction Plot for Water Test with No Mixer at 30°C

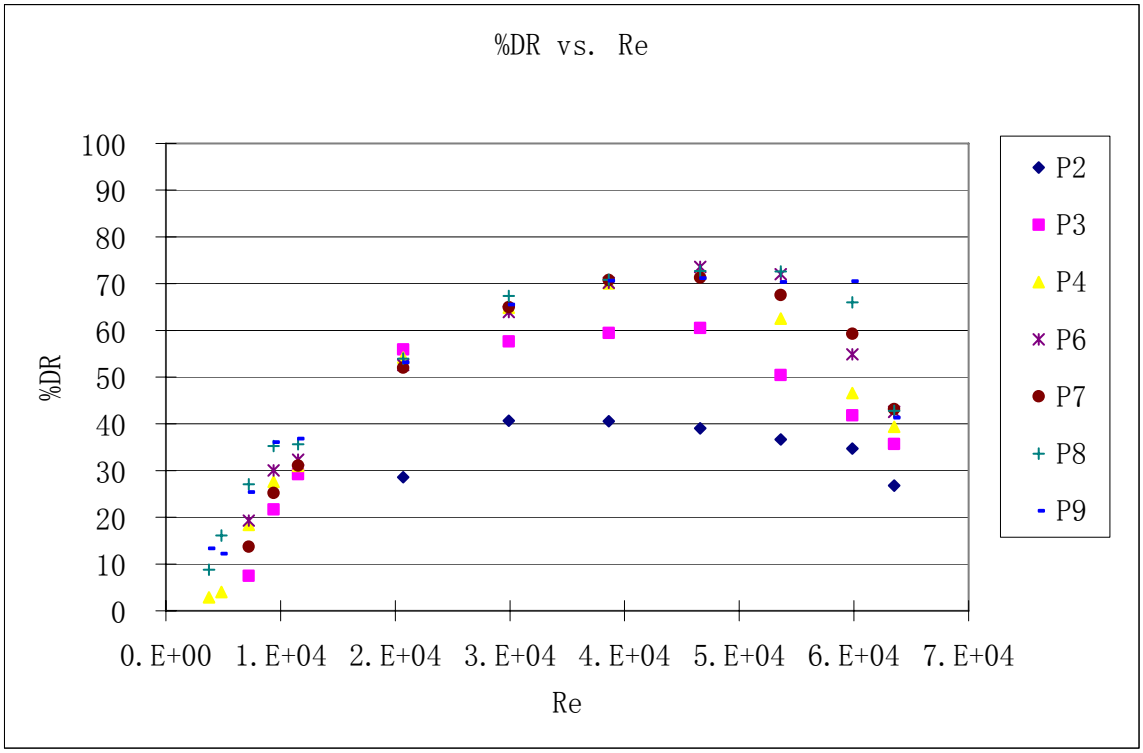

Figure 23: Percent Drag Reduction Plot for Drag Reducing Solution Test with No Mixer at 30°C

At all temperatures, the surfactant solution is clearly an effective drag reducing agent. No transducer (excluding P5) showed a percent drag reduction greater than 5% for water at any temperature. The high percent drag reduction shown in water tests at low flow rates is due to the deviation from the von Karman line discussed earlier, which is caused by a lack of fully developed turbulent flow. Each transducer showed surfactant drag reducing behavior at turbulent flows with only P2 showing a significantly lower drag reduction, which is to be expected because that section of pipe has a diameter change that imparts shear stress into the flow. This shear stress may cause some of the micelles to break up, reducing the drag reduction effect. Effective drag reduction is usually defined as 50% and above, which almost every surfactant data point showed

under turbulent flow conditions. The maximum percent drag reduction was anywhere from 75%-80% depending on the main loop temperature.

The data collected also show that the surfactant drag reducing solution shows much lower heat transfer compared to water at the same temperature. Figures 24, 25, and 26 below show this reduction by plotting inner wall heat transfer coefficient against Reynolds number. The data clearly show that the heat transfer of the drag reducing solution is greatly reduced compared to that of water at the same temperature. The average percent heat transfer reductions were 90%, 81%, and 84%, while the maximum values were 97%, 89%, and 90%, for main loop temperatures of 10°C, 20°C, and 30°C, respectively.

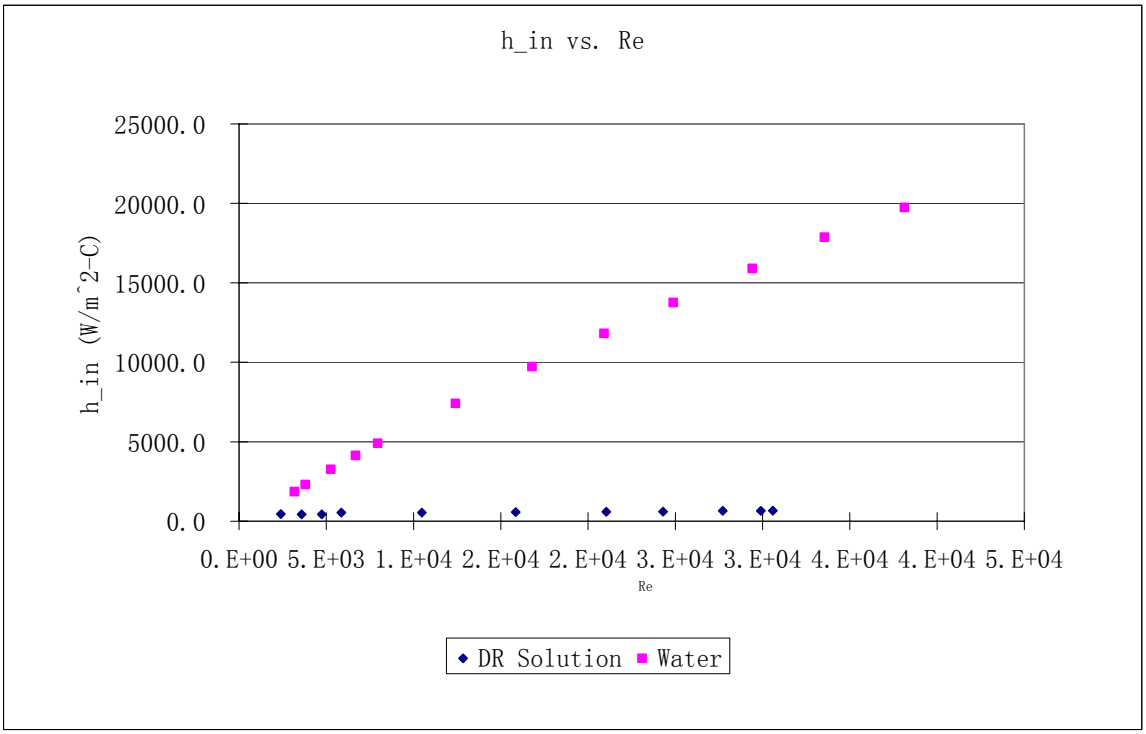

Figure 24: Heat Transfer Coefficient Plot for Drag Reducing Solution and Water with No Mixer at 10°C

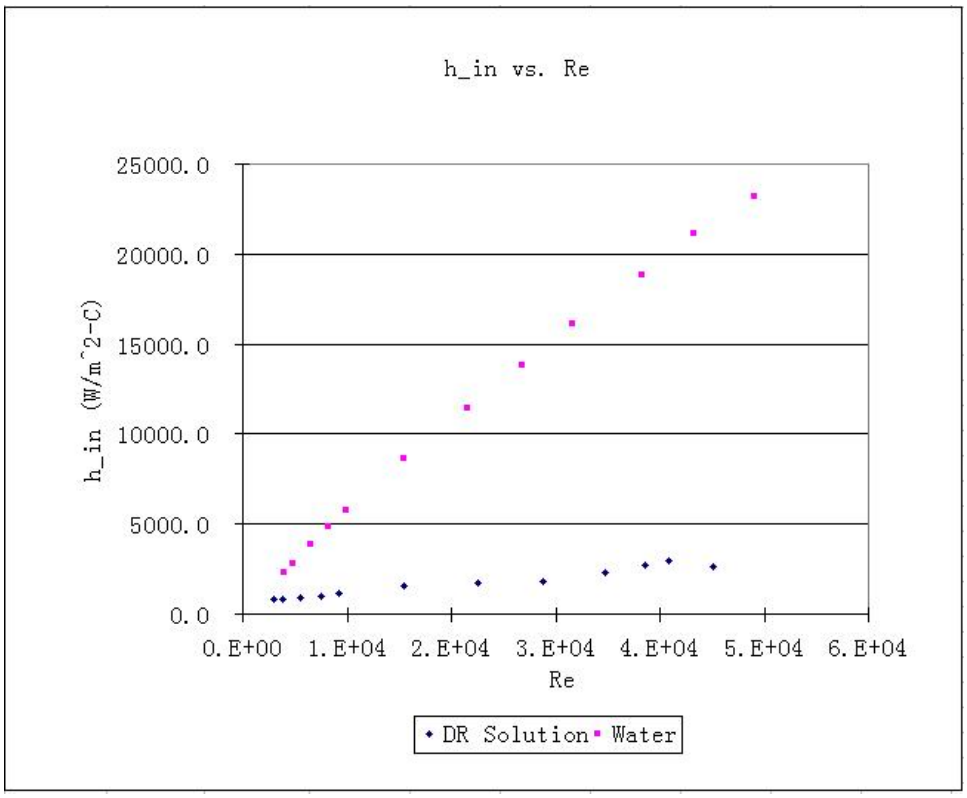

Figure 25: Heat Transfer Coefficient Plot for Drag Reducing Solution and Water with No Mixer at 20°C

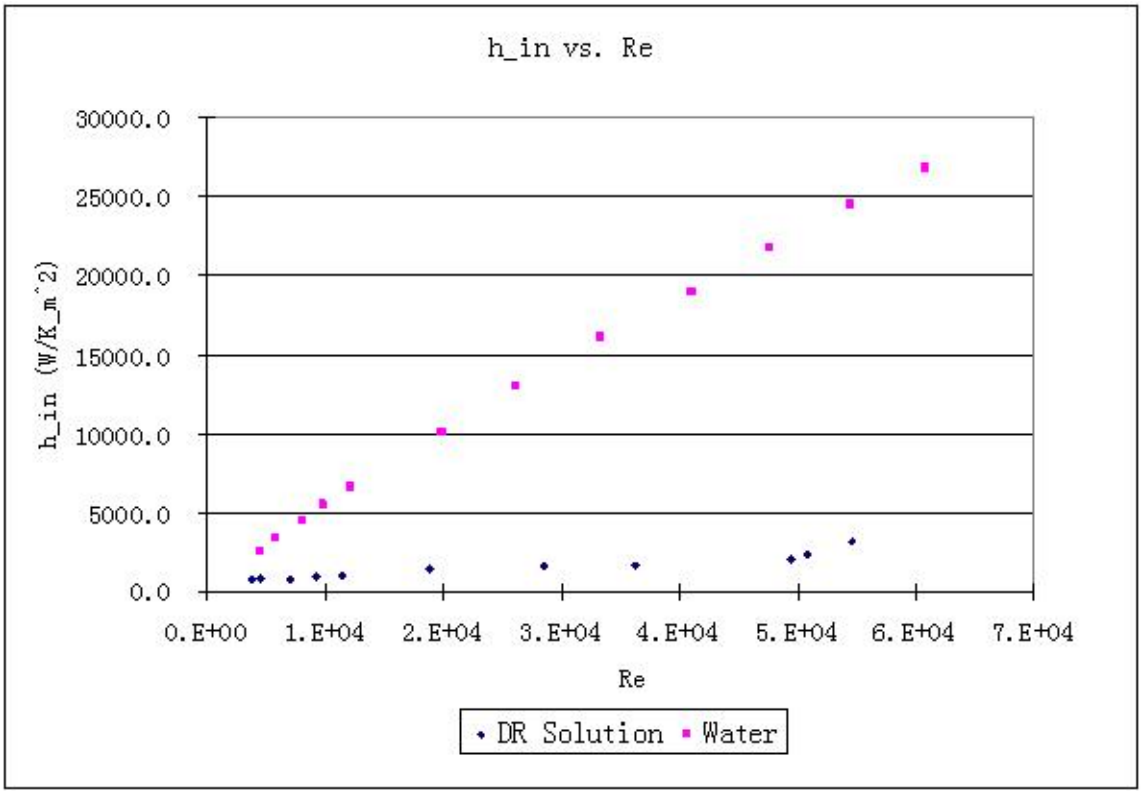

Figure 26: Heat Transfer Coefficient Plot for Drag Reducing Solution and Water with No Mixer at 30°C

The data in Figure 27 show that the percent heat transfer reduction is always greater than the percent drag reduction. This means the ratio of percent heat transfer reduction to percent drag reduction is greater than one as noted by Aguilar, et al[15]. Before turbulent flow is developed, the ratio is higher due to decreased percent drag reduction.

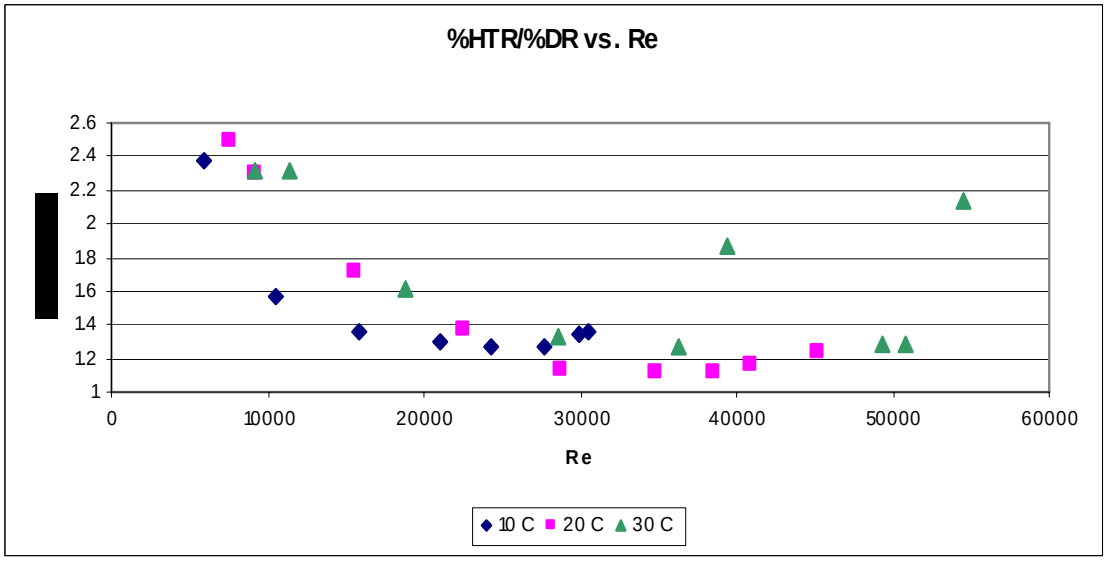

Figure 27: %HTR to %DR Ratio vs. Reynolds Number for Drag Reducing Solution with No Mixer at 10°C, 20°C, and 30°C

In order to show that the surfactant solution loses its drag reducing capabilities after coming into contact with a static mixer but then regains them downstream, plots of percent drag reduction at different downstream locations are shown below. Figures 28, 29, and 30 show the plots for the solution with no mixer, one mixer length, and three mixer lengths, respectively, all at 10°C. With no mixer, the solution shows effective drag reduction (≥50%) across all pressure transducers, except for P2, which was marginal. When the static mixers are added, however, the first transducer downstream of the mixer, P2, shows almost total loss of drag reduction capability as expected. Further

downstream, however, the solution regained its drag reduction properties as the surfactant self-assembled its micellar structure. Every other transducer from P3-P9 measured a percent drag reduction over 90% of the value found without any mixer. This behavior was essentially mirrored by the test run with three static mixer lengths.

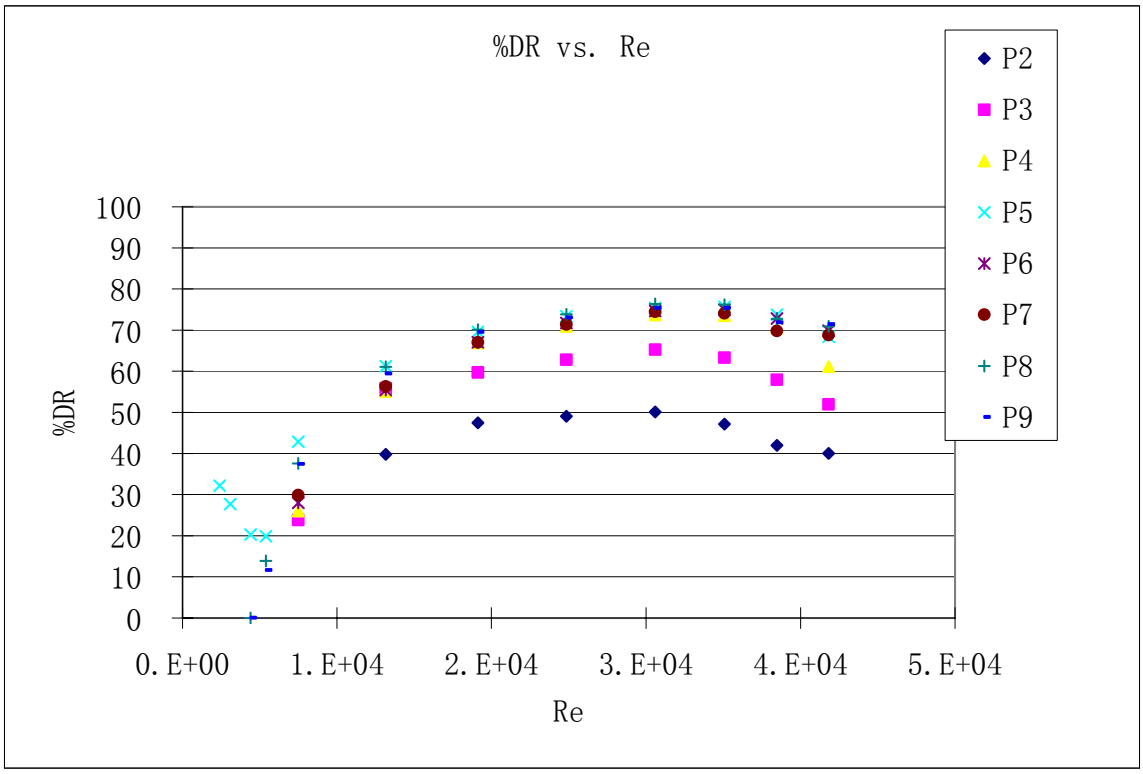

Figure 28: Percent Drag Reduction Plot for Drag Reducing Solution with No Mixer at 10°C

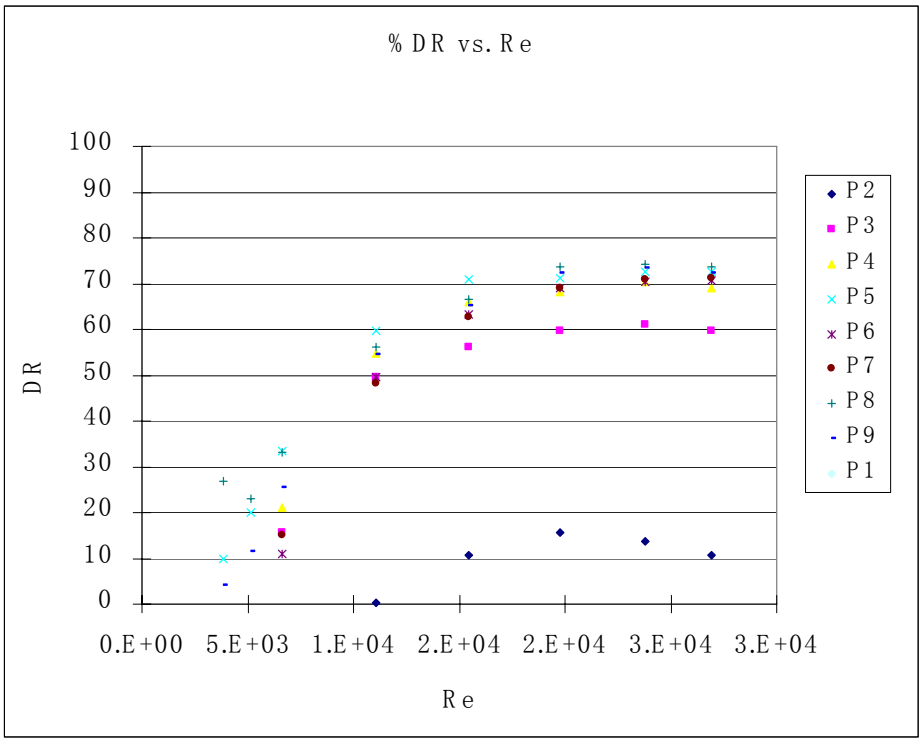

Figure 29: Percent Drag Reduction Plot for Drag Reducing Solution with 1 Static Mixer Length at 10°C

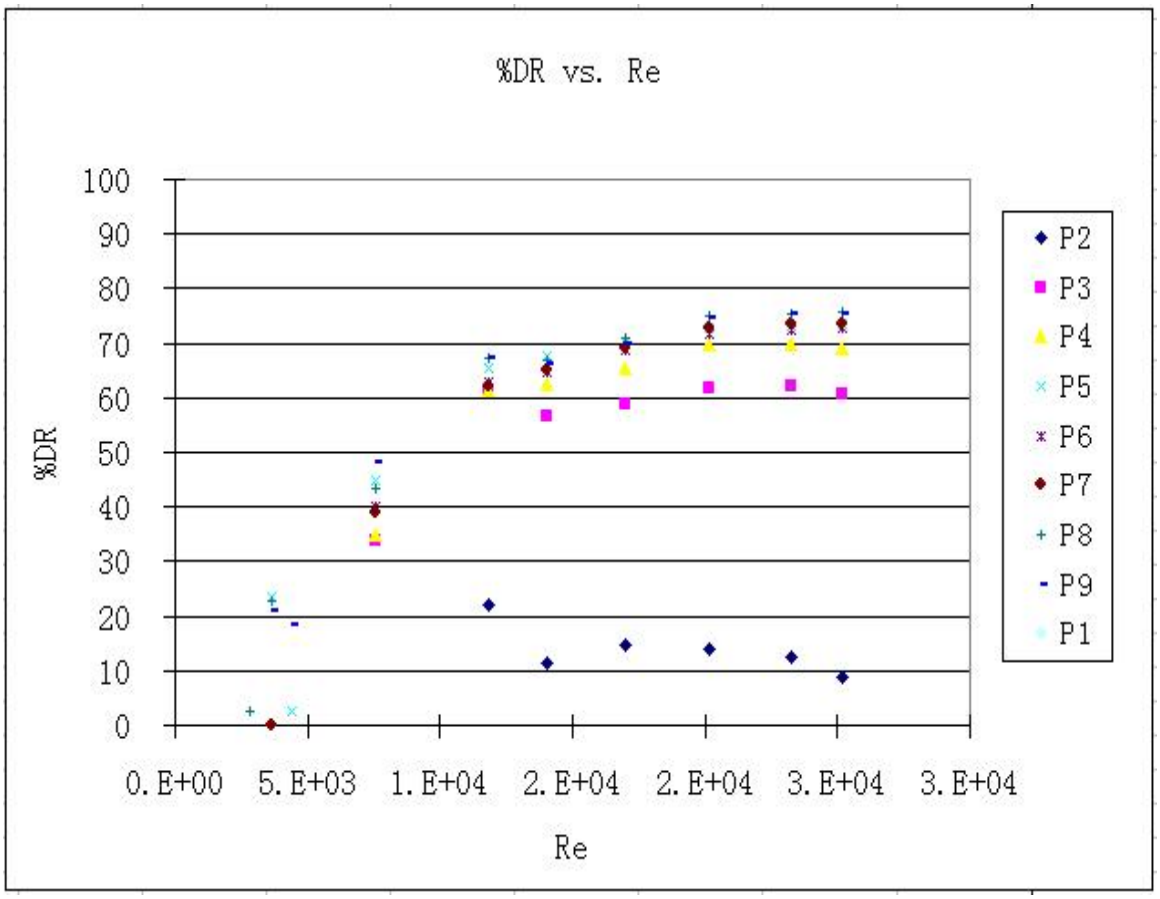

Figure 30: Percent Drag Reduction Plot for Drag Reducing Solution with 3 Static Mixer Lengths at 10°C

These results can be used to determine the recovery time of the solution as described in the data reduction section. Table 3 gives an example of the data table for these calculations for a drag reduction test for the solution with one mixer length at 10°C. Only data points under turbulent flow were considered. Table 4 shows the average recovery times for each of the drag reducing solution tests done with mixer lengths installed. It shows that the increase in mixer length causes a longer recovery time, which would be expected since the micellar structure is degraded more in the longer mixer. The surprising result, however, is that the recovery time increases with temperature. The higher temperature gives faster molecular movement, which should lead to faster self-assembly times, but this is apparently not the case for this surfactant.

Table 3: Example of Recovery Time Calculation Table

Re	Velocity (m/s)	Recovery Point	Recovery Time (s)
15485.59	1.22	P3	2.2
22402.39	1.77	P4	2.0
29246.89	2.31	P4	1.5
34120.28	2.69	P5	1.6
38479.60	3.03	P5	1.4
43282.15	3.41	P8	2.0
45209.04	3.56	P7	1.7
Average			1.8

Table 4: Average Recovery Times for Surfactant Solution

Mixer Length	Temperature (°C)	Average Recovery Time (s)
1	10	1.5
1	20	1.5
1	30	1.8
3	10	1.7
3	20	1.9
3	30	2.1

The next goal is to determine whether the presence of one or more static mixers at the entrance to heat exchanger 1 improved the heat transfer properties of the system. Figures 31, 32, and 33 show plots of the inner wall heat transfer coefficient for the drag reducing solution with no mixer, one mixer length, and three mixer lengths at one temperature on one plot. At 10°C, one mixer length showed an average heat transfer improvement of 480% and a maximum of 970%, while three mixer lengths had an average improvement of 430% and a maximum of 1000%. At 20°C, one mixer length showed an average heat transfer improvement of 50% and a maximum of 130%, while three mixer lengths had an average improvement of 65% and a maximum of 165%. At

30°C, one mixer length had an average heat transfer improvement of 175% and a maximum of 440%, while three mixer lengths had an average improvement of 130% and a maximum of 375%. The data show that the addition of the static mixers does considerably improve the heat transfer properties of the system; however, when the mixer length is increased, there is not always a corresponding increase in heat transfer. In fact, sometimes there is a slight decrease in percent heat transfer increase. The data for the three static mixer length tests are erratic, however, so further investigation should be done before firm conclusions are reached. The three mixer length tests were also not able to reach the highest Reynolds numbers because of the large pressure drop across the mixer. The largest heat transfer increases were seen at the largest Reynolds numbers, so this may affect the averages and maximum values for three mixer lengths.

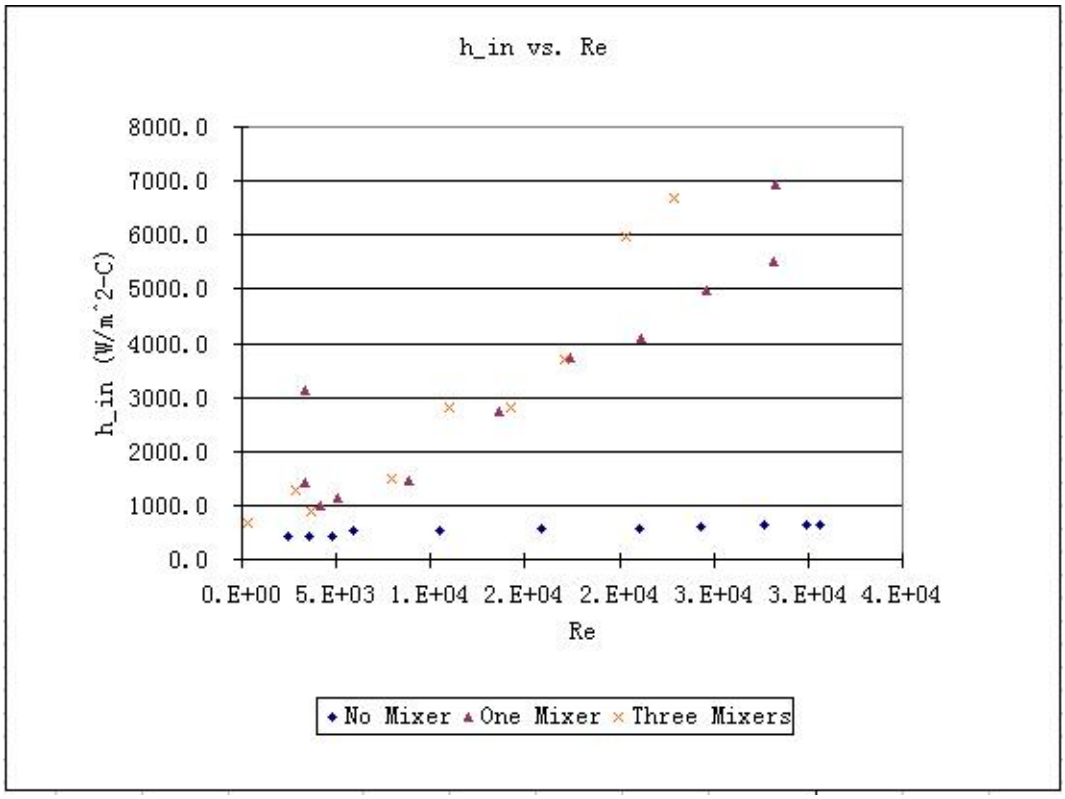

Figure 31: Heat Transfer Coefficient Plot for Drag Reducing Solution at 10°C

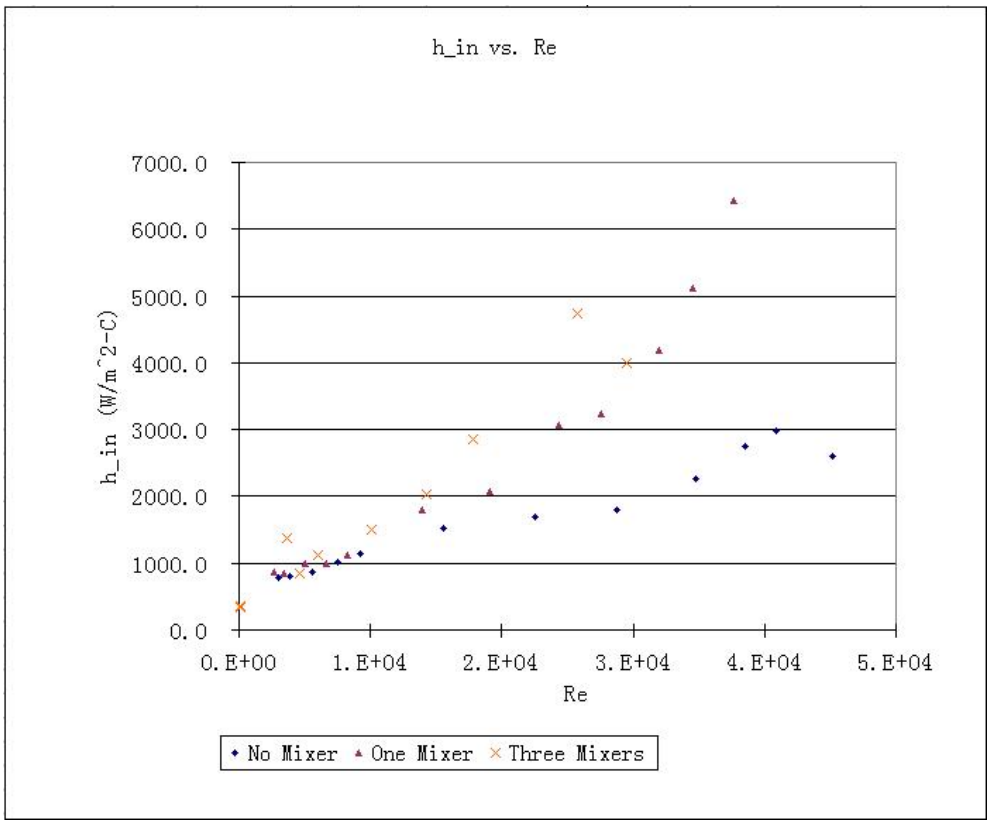

Figure 32: Heat Transfer Coefficient Plot for Drag Reducing Solution at 20°C

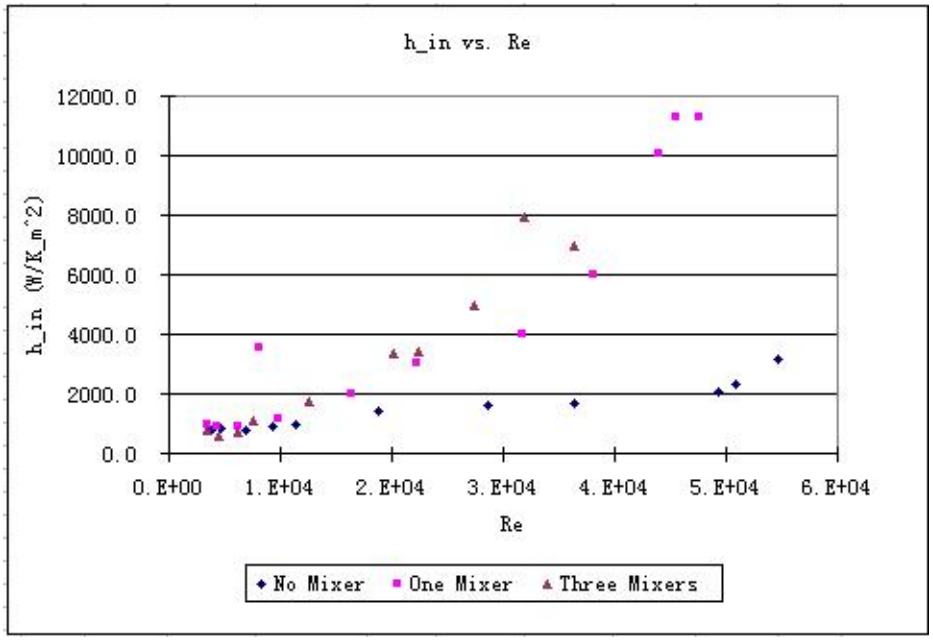

Figure 33: Heat Transfer Coefficient Plot for Drag Reducing Solution at 30°C

The final goal is to investigate the pressure drop penalty incurred by the static mixer addition. An obstruction in the piping causes an increased pressure drop, which would negate some of the drag reduction energy savings. Figure 34 shows the pressure drop across the static mixer piping section, P1, for water drag reduction tests at 20°C for various mixer lengths. The data clearly shows a massive increase in pressure drop with increasing mixer length. Adding one mixer length gives a pressure drop maximum of 46 psi and shows an average increase of 1875% from the data with no mixer. When the length is increased to three lengths, the maximum value climbs to 77 psi, which is not even at the maximum flow rate, and the average increase is more than 4000% over the data with no mixer.

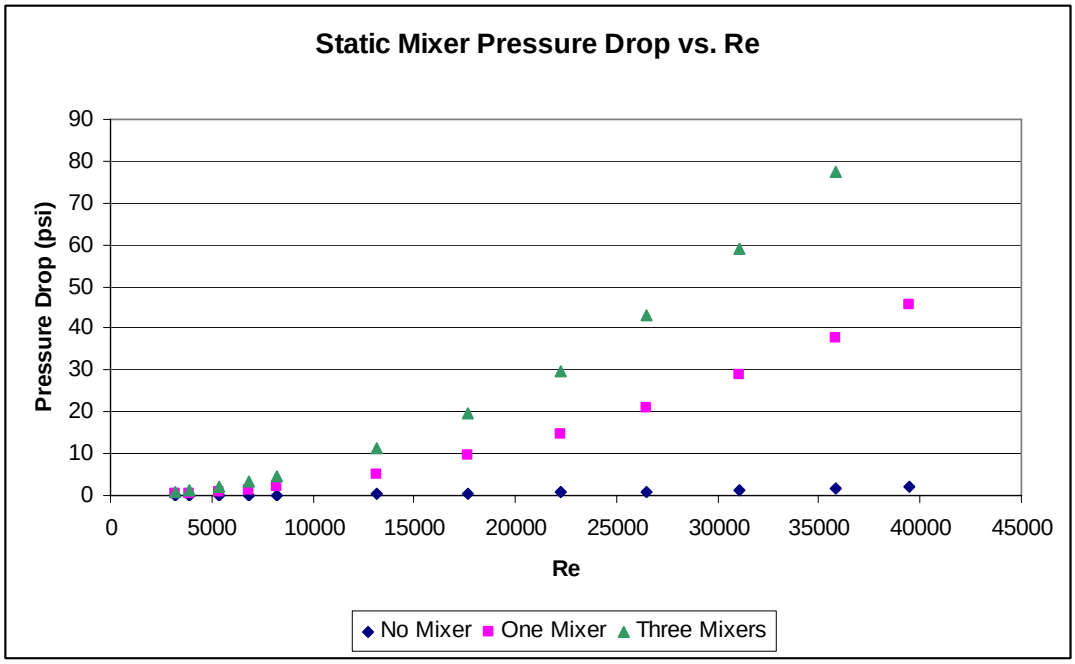

Figure 34: Static Mixer Pressure Drop vs. Reynolds Number at 20°C and All Mixer Lengths

Conclusions

The goal of this research was to investigate whether the addition of static mixers to a surfactant drag reducing solution would enhance heat transfer in a tube-in-tube heat exchanger. Drag reduction and heat transfer tests were run in a pipe flow system under various conditions. The variables were the primary loop fluid, the primary loop temperature, the Reynolds number, and the length of static mixer at the entrance to the main heat exchanger. Calculations were performed on the data to determine the friction factor, percent drag reduction, amount of heat transferred, inner wall heat transfer coefficient, and Nusselt number for each of the experimental runs. After analyzing the data, the following conclusions can be made:

1. A solution of water, 5.0 mM tris (2-hydroxyethyl) tallow ammonium acetate, and 12.5 mM sodium salicylate is an effective drag reducing agent. The maximum percent drag reduction found in these tests was 80%.
2. The surfactant drag reducing solution is a poor heat transfer fluid under normal flow conditions. It suffers a heat transfer reduction of at least 80% at all system temperatures tested.
3. As shown in other literature, the percent heat transfer reduction is always greater than the percent drag reduction. The ratio for individual tests usually fell into the range of 1.1-1.4 at Reynolds numbers above 10,000.
4. The addition of a static mixer alters the micellar structure of the solution, causing it to temporarily lose its drag reduction capabilities and reduce its heat transfer reduction.

5. The surfactant solution is able to regain its drag reduction properties downstream of the static mixer through self-assembly. The recovery times varied from 1.5-2.1 seconds. It increased with increasing mixer length, but also with increasing temperature, which was not expected.
6. When a static mixer is placed at the entrance of a heat exchanger, the heat transfer properties of the drag reducing solution are greatly enhanced. The largest percentage gain (400+%) was seen at a main loop temperature of 10°C, while 20°C (~55%) and 30°C (~150%) showed more moderate gains.
7. Lengthening the static mixer did not necessarily increase the heat transfer gains. In fact, at 10°C and 30°C the longer mixer led to decreased heat transfer performance.
8. The longer static mixer had a significantly larger pressure drop penalty. One mixer length caused an increased pressure drop of 1875%, while the three mixer lengths had an increase of over 4000%.

Recommendations

While the results of this investigation showed that static mixers can enhance the heat transfer properties of surfactant drag reducing solutions in tube-in-tube heat exchangers, more research needs to be done.

1. In order to obtain the best data, more accurate thermocouples could be utilized in the heat transfer experiments. The four most important locations for these thermocouples are the inlet and outlet flows of both the primary and heat transfer fluid in heat exchanger 1.
2. For greater accuracy, the experiments should be rerun with improved thoroughness and a greater attention to the data being collected. For example, more time could be taken to ensure that the data points produced are reliable before moving on to the next data point.
3. The experiments should also be run at a wider range of temperatures as well because some of the surfactant behavior is temperature dependent, so those boundaries should be explored further.
4. In order to have the primary loop fluid serve as the higher temperature fluid in heat exchanger 1, a new heating device with greater control would be required.
5. The surfactant behavior can also be time dependent as well, so experiments should be designed and executed to investigate whether the results obtained in this study would be the same at longer time scales.
6. The final recommendation is to incorporate other designs of static mixers into the experiments. Size, material, shape, and design and their effect on heat transfer enhancement should all be investigated further.

References

1. Mysels, K. J., Flow of thickened fluids. 2492173, 1949.
2. Toms, B. A., The flow of linear polymer solutions through straight tubes at large Reynolds numbers. *Proceedings of the International Rheological Congress (General and Physical Chemistry)* 1949, II; III, 135-141; 47-49, 51-52.
3. Harwigsson, I.; Hellsten, M., Environmentally acceptable drag-reducing surfactants for district heating and cooling. *Journal of the American Oil Chemists' Society* 1996, 73, (7), 921-928.
4. Dujmovich, T.; Gallegos, A., Drag reducers improve throughput, cut costs. *Offshore* 2005, 65, (12), 1-4.
5. Dembek, G.; Bewersdorff, H. W., Short-time increase of sewer capacity by addition of water-soluble polymers. *GWF, Wasser/Abwasser* 1981, 122, (9), 392-395.
6. Fabula, A. G., Fire-fighting benefits of polymeric friction reduction. *Journal of Basic Engineering* 1971, 93, (3), 453-455.
7. Mostardi, R. A.; Thomas, L.C.; Greene, H. L.; Van Essen, F.; Nokes, R. F., Suppression of atherosclerosis in rabbits using drag reducing polymers. *Biorheology* 1978, 15, (1), 1-14.
8. Burger, E. D.; Munk, W. R.; Wahl, H. A., *Journal of Petrochemical Technology* 1982, (2), 377-386.
9. Manfield, P. D.; Lawrence, C. J.; Hewitt, G. F., Drag reduction with additives in multiphase flow: a literature survey. *Multiphase Science and Technology* 1999, (11), 197-221.

10. Qi, Y.; Weavers, L. K.; Zakin, J. L., Enhancing heat-transfer ability of drag reducing surfactant solutions with ultrasonic energy. *Journal of Non-Newtonian Fluid Mechanics* 2003, 116, 71-93.
11. Fontaine, A. A.; Deutsch, S.; Brungart, T. A.; Petrie, H. L.; Fenstermachker, M., Drag reduction by coupled systems: microbubble injection with homogenous polymer and surfactant solutions. *Experiments in Fluids* 1999, (26), 397-403.
12. Shenoy, A. V., A review on drag reduction with special reference to micellar systems. *Colloid and Polymer Science* 1984, 262, (4), 319-337.
13. Kostic, M., On turbulent drag and heat transfer reduction phenomena and laminar heat transfer enhancement in non-circular duct flow of certain non-Newtonian fluids. *International Journal of Heat and Mass Transfer* 1994, 37, (1), 133-147.
14. Dimant, Y; Poreh, M., Heat transfer in flows with drag reduction. *Advanced Heat Transfer* 1976, 12, 77-113.
15. Aguilar, G.; Gasljevic, K.; Matthys, E. F., Coupling between heat and momentum transfer mechanism for drag-reducing polymer and surfactant solutions. *Journal of Heat Transfer* 1999, 121, 796-802.
16. Zakin, J. L.; Lu, B.; Bewersdorff, H. W., Surfactant drag reduction. *Reviews in Chemical Engineering* 1998, 14, (4-5), 253-320.
17. Qi, Y.; Kawaguchi, Y.; Christensen, R. N.; Zakin, J. L., Enhancing heat transfer ability of drag reducing surfactant solutions with static mixers and honeycombs. *International Journal of Heat and Mass Transfer* 2003, 46, 5161-5173.
18. Qi, Y.; Kawaguchi, Y.; Lin, Z.; Ewing, M., Christensen, R. N.; Zakin, J. L., Enhanced heat transfer of drag reducing surfactant solutions with fluted tube-in-

tube heat exchanger. *International Journal of Heat and Mass Transfer* 2001, 44, 1495-1505.

19. Qi, Y., Investigation of relationships among microstructure, rheology, drag reduction, and heat transfer of drag reducing surfactant solutions, Ph.D. Dissertation, The Ohio State University, Columbus, Ohio, 2002.
20. Jakob, M., Heat Transfer. John Wiley & Sons. New York. 1949. 550-554.
21. Foust, A. S.; Wenzel, L. A.; Clumb, C. W.; Maus, L.; Anderson, L. B., Principles of Unit Operations. John Wiley & Sons. New York. 1967. 168-169.